REVIEW

Nucleate and transition boiling heat transfer under pool and external flow conditions

V. K. Dhir
Mechanical, Aerospace and Nuclear Engineering Department, School of Engineering and Applied Science, University of California, Los Angeles, Los Angeles, CA, USA

In this paper an overview of the boiling process, including recent advances made toward a mechanistic understanding of nucleate and transition boiling, is presented. Out of necessity, the review does not include boiling on enhanced surfaces or boiling of mixtures. Discussion of film boiling is also not included, as it is the subject of another review article. Only pool and external flow boiling of ordinary liquids are discussed. A few comments are made with respect to the theoretical and experimental studies that should be made in the future to further our understanding of the boiling process.

Keywords: pool boiling; flow boiling; nucleate boiling; maximum heat flux; transition boiling

Introduction

Studies of boiling and two-phase flow and heat transfer continue to represent a significant fraction of the publications that appear in archival journals, proceedings of conferences, and symposia volumes. Two of the reasons for the continued strong interest in boiling heat transfer, since the first boiling curve was obtained by Nukiyama[1] more than half a century ago, are as follows:

(1) Boiling is a very efficient mode of heat transfer and as such is employed in component cooling and in various energy conversion systems. The quest for improvement in the performance of the equipment and the demand imposed by new high density energy systems continue to motivate studies on boiling heat transfer.
(2) Boiling is an extremely complex and illusive process that continues to baffle and challenge inquisitive minds.

Unfortunately, for a variety of reasons, fewer studies have focused on the physics of the boiling process than have been tailored to fit the needs of engineering endeavors. As a result. the literature has been flooded with the correlations involving several adjustable parameters. These correlations can provide quick input to design, performance, and safety issues and hence are attractive on a short-term basis. However, the usefulness of the correlations diminishes very rapidly as parameters of interest start to fall outside the range of physical parameters for which the correlations were developed. Also, correlations involving several empirical constants tend to cloud the physics. Thus, if we wish to reduce the repetition of experimental effort in response to changes in the physical parameters of interest in an engineering enterprise, it is important to place greater emphasis on the fundamental understanding of the process. A persistent effort in this direction will go a long way in transforming studies of boiling heat transfer from an art to a science and would be attractive and exciting to new researchers.

Address reprint requests to Professor Dhir at the Mechanical, Aerospace and Nuclear Engineering Department, School of Engineering and Applied Science, University of California at Los Angeles, Los Angeles, CA 90024-1597, USA.

Received 11 April 1991; accepted 28 June 1991

In this paper recent studies on nucleate and transition boiling processes are reviewed. Similar reviews have appeared in the literature in the past, as for example, those by Kenning[2] and Fujita.[3] In this paper comments are made reflecting the author's perception of what needs to be done to advance the state of knowledge. Though an attempt was made to include as many recent investigations as possible, the list of citations may not be exhaustive. For this the author apologizes.

Nucleate boiling

The first mode of heat transfer to appear with the increase of heat flux at a surface initially in thermal equilibrium with the host liquid is convection. The convective flow can be due either to buoyancy or to imposed pressure difference along or across the surface. With further increase in the surface temperature or heat flux, bubbles appear randomly on the heated surface. In the late 1950s, which was one of the most exciting periods for boiling heat transfer research, Bankoff[4] was the first one to show theoretically that cavities, pits, and scratches on the heater surface are the preferred sites for bubbles. A year later, Clark et al.[5] showed experimentally that this is indeed the case. Once it was clear that the bubbles formed on the so-called dark holes on the heater surface, the next challenge was to predict the superheat or heat flux at which boiling inception occurred.

Inception

One of the first attempts to provide a quantitative criterion for prediction of inception superheat was made by Hsu.[6] According to Hsu's criterion, a vapor embryo occupying a cavity will grow into a bubble if the liquid temperature at the tip of the embryo is at least equal to the saturation temperature corresponding to the pressure in the bubble. If cavities of all sizes containing a vapor embryo are available, the size of the cavity that will nucleate first is obtained by applying Hsu's criterion as

$$D_c = \frac{\sqrt{8 f_1(\phi)^2 T_{sat}\,\delta\sigma}}{f_2(\phi)\rho_G h_{LG}\,\Delta T} \qquad (1)$$

where δ is the thickness of the equivalent conductive thermal layer, and $f_1(\phi)$ and $f_2(\phi)$ depend on the embryo shape, which in turn depends on the contact angle ϕ. For a contact angle of 90° both f_1 and f_2 are equal to unity. The corresponding heat flux is related to the wall superheat as

$$q = \frac{h_{LG}\rho_G k_L}{8 f_2(\phi)\sigma T_{sat}} (\Delta T)^2 \tag{2}$$

Generally, the size of the largest cavity available on a surface is smaller than that given by Equation 1 and consequently the incipience heat flux or wall superheat is larger than that given by Equation 2.

In terms of the size of the largest cavity available on the surface, the incipience heat flux can be written as

$$q = \frac{2 f_1 k_L \Delta T}{f_2 (D_2)_{max}} - \frac{8 f_1^2 \sigma T_{sat} k_L}{f_2 \rho_G h_{LG} (D_c)^2_{max}} \tag{3}$$

Equation 3 represents one equation in two unknowns, namely q and ΔT. To solve explicitly for both, we need another relation between q and ΔT. This relation is provided by natural or forced convection. Equation 3 is very general and can be used to determine the size of a cavity that will nucleate at a given heat flux and wall superheat such that

$$D_c = \frac{\dfrac{4 f_1 \sigma T_{sat}}{\rho_G h_{LG} \Delta T}}{\left[1 - \dfrac{f_2 D_c q}{f_1 2 k_L \Delta T}\right]} \tag{4}$$

Equations 3 or 4 do a reasonable job in predicting the data obtained under well-defined conditions, as was demonstrated by Hsu and Graham.[7] However, large deviations are possible if cavities of size D_c are completely filled with liquid or if the interface of the vapor embryo represents a stable equilibrium condition with the superheated liquid. Mizukami[8] and Nishio[9] have shown that if the curvature of the interface increases with increase in vapor volume, the interface will be stable and may not lead to an active site. Changes in thermal conditions, noted by Kenning,[10] and flow conditions in the vicinity of the wall, as well as interaction between sites, can lead to activation of inactive sites and deactivation of active sites. At very low heat fluxes, induced activation and delayed deactivation of a reentrant cavity can manifest themselves in the form of hysteresis in the boiling curve. This behavior is prominent in liquids that wet the surface well. For these liquids, large cavities are generally flooded. As a result the convective process continues to persist up to higher wall superheats. Activation of a large number of cavities either by induction or otherwise can, in a heat flux controlled procedure, lead to a sudden improvement in heat removal, and in turn, to a reduction in wall superheat.

At low heat fluxes the second term in the denominator in Equation 4 is generally much less than unity and thus can be neglected. With this assumption, the size of a nucleating cavity varies inversely with wall superheat. In fact, this is the assumption employed by Mikic and Rohsenow[11] in their model for nucleate boiling heat transfer, which will be elaborated on further. However, the assumption leads to unrealistic results

Notation

a	Thermal diffusivity
D_s	Diameter of the largest cavity present on the surface
c_p	Specific heat
D	Bubble or disk diameter
D_c	Cavity diameter
D_d	Bubble diameter at departure
D_o	Vapor stem diameter
d	Jet diameter
F	Fractional area of the heater
Fr	Froude number
f	Frequency
Gr	Grashof number
g	Gravitational acceleration
h	Heat transfer coefficient
h_{LG}	Latent heat of vaporization
h_{nc}	Natural convection heat transfer coefficient
Ja	Jakob number
k	Thermal conductivity
L	Characteristic length
L'	Dimensionless characteristic length
N_a	Activity cavity site density
N_s	Site density of cavities present on a surface
N_{max}	Maximum site density of active cavities present on the surface
Nu	Nusselt number
P	Pressure
P^*	Reduced pressure
Pe	Peclet number
Pr	Prandtl number
q	Heat flux
S	Separation distance between active cavities
T	Temperature
T_b	Bulk temperature
T_{sat}	Saturation temperature
T_w	Wall temperature
t	Time
t_0	Duration of transient
U	Superficial velocity
We	Weber number
x	Distance normal to heater surface
z	Distance along heater surface

Greek symbols

α	Void fraction
β	Liquid accessibility parameter or coefficient of isobaric expansion
δ	Thermal layer thickness
θ	Angle of inclination
μ	Viscosity
ρ	Density
σ	Surface tension
ϕ	Contact angle

Subscripts

c	Cooling
DNB	Departure from nucleate boiling
G	Vapor/gas
h	Heating
L	Liquid
M	Measured
max	Maximum
min	Minimum
sub	Subcooled
P	Predicted
st	Steady state
stD	Steady-state DNB

at high heat fluxes when the thickness of the thermal layer adjacent to the heated surface is comparable to the size of the nucleating cavity. Also in such a situation it is more appropriate to use a nonlinear temperature profile in the thermal layer.

Bubble growth and departure

After inception, a bubble continues to grow (in a saturated liquid) until forces causing it to detach from the surface exceed those pushing the bubble against the wall. Generally two points of view with respect to growth of a bubble on a heated surface have been put forth in the literature. One group of investigators has proposed that the growth of the bubble occurs as a result of evaporation all around the bubble interface. The energy for evaporation is supplied from the superheated liquid layer that surrounds the bubble since its inception. Bubble growth models similar to that proposed for growth of a vapor bubble in a sea of superheated liquid, such as that of Plesset and Zwick,[12] have been proposed. The bubble growth process on a heater surface, however, is more complex because the bubble shape changes continuously during the growth process and superheated liquid is confined to only a thin region around the bubble. Mikic et al.[13] using a geometric factor to relate the shape of a bubble growing on a heated surface to a perfect sphere, and properly accounting for the thermal energy that is stored in the liquid layer prior to bubble inception, obtained an analytical solution for the bubble growth rate. Their expression for the growth rate is

$$\frac{dD^*}{dt^*} = 2\left[t^* + 1 - \theta\left(\frac{t^*}{t^* + t_w^*}\right)^{1/2}\right]^{1/2} - t^{*1/2} \tag{5}$$

where

$$D^* = \left(\frac{b\rho_G \Delta T h_{LG}}{\rho_L T_{sat}}\right)^{1/2}\left(\frac{\pi D}{12 a_L \mathrm{Ja}^2}\right) \tag{6}$$

$$t^* = \left(\frac{pbG\,\Delta T h_{LG}}{\rho_L T_{sat}}\right)\left(\frac{\pi t}{12 a_L \mathrm{Ja}^2}\right) \tag{7}$$

$$\theta = \frac{T_w - T_b}{\Delta T} \tag{8}$$

and

$$\mathrm{Ja} = \frac{\rho_L c_{PL} \Delta T}{\rho_G h_{LG}} \tag{9}$$

In Equation 8, T_b is the liquid bulk temperature and in Equations 6 and 7 b is a geometric parameter that has a value of two thirds for a perfect sphere.

The second point of view is that most of the evaporation occurs at the bubble base and that the micro/macrolayer between the vapor-liquid interface and the heater surface plays an important role. Snyder and Edwards[14] were the first to propose this mechanism for evaporation. Subsequently, Moore and Mesler[15] deduced the existence of a microlayer under the bubble from the oscillations in the temperatures measured at the bubble release site.

The diameter to which a bubble grows before departing is dictated by the balance between forces that act on the bubble. Fritz[16] correlated the bubble departure diameter by balancing buoyancy, which acts to lift the bubble from the surface, with surface tension force, which tends to hold the bubble to the wall so that

$$D_d = 0.0208\phi\sqrt{\frac{\sigma}{g(\rho_L - \rho_G)}} \tag{10}$$

where ϕ is the contact angle measured in degrees. Though significant deviations with respect to the above equation have been reported in the literature, especially at high pressures, Equation 10 does provide a correct length scale for the boiling process. Several other expressions that are obtained either empirically or analytically by involving various forces acting on a bubble have been reported in the literature for bubble departure diameter. These expressions, however, are not always consistent with each other. Some investigators report an increase in bubble diameter at departure with wall superheat, whereas others find the bubble diameter at departure to be insensitive to, or decrease with, wall superheat. Also, there exists a small controversy with respect to the role of various forces. Contrary to the commonly held view, the work of Cooper et al.[17] suggests that surface tension may assist bubble departure. Cole and Rohsenow[18] correlated bubble diameter at departure at low pressures as

$$D_d = 1.5 \times 10^{-4}\sqrt{\frac{\sigma}{g(\rho_L - \rho_G)}}\,\mathrm{Ja}^{*5/4} \text{ for water} \tag{11}$$

and

$$D_d = 4.65 \times 10^{-4}\sqrt{\frac{\sigma}{g(\rho_L - \rho_G)}}\,\mathrm{Ja}^{*5/4} \text{ for other liquids} \tag{12}$$

where

$$\mathrm{Ja}^* = \frac{\rho_L c_{PL} T_{sat}}{\rho_G h_{LG}} \tag{13}$$

Gorenflo et al.[19] have modified the equation proposed earlier by Moalem et al.[20] and Cole and van Stralen[21] to obtain an expression for bubble departure diameter at high heat fluxes as

$$D_d = C_1\left(\frac{\mathrm{Ja}^4 a_L^2}{g}\right)^{1/3}\left[1 + \left(1 + \frac{2\pi}{3\mathrm{Ja}}\right)^{1/2}\right]^{4/3} \tag{14}$$

Different values of C_1 were used for different liquids.

Knowing the growth rate and the diameter to which a bubble grows before departing, the growth time, t_g, can be calculated. After bubble departure, cold pool liquid fills the space vacated by the bubble. Schlieren pictures by Hsu and Graham[7] show that an area about two times the bubble diameter at departure is influenced by bubble motion. As a result, the thermal layer reforms over an area of a circle of diameter $2D_d$ surrounding the nucleation site. A new bubble at this location will now grow until the superheated liquid layer is reestablished and the inception criterion is satisfied. The time taken by the thermal layer to develop prior to inception is termed the waiting period. Han and Griffith[22] obtained an analytical expression for the waiting period by assuming the liquid layer to be semi-infinite as

$$t_w = \left[\frac{f_2 D_c}{2\sqrt{\pi a_L} f_1\left[1 - \dfrac{4 f_1 \sigma T_{sat}}{\Delta T \rho_G h_{LG} D_c}\right]}\right]^2 \tag{15}$$

It can be seen that the waiting period is a dual function of D_c. The waiting time will first decrease and then increase with cavity size; however, it will continuously decrease as the wall superheat is increased.

Conceivably, a theoretical evaluation of the bubble release frequency can be made from expressions for the waiting time, t_w, and the growth time, t_g. In fact, such an approach meets with little success when a comparison is made with the data. Some of the reasons for the discrepancy are the following:

(1) Evaporation takes place at the base and at the surface of the bubbles, and the growth models reported in the literature do not account for both.

(2) Generally large cavities yield large bubbles. This in turn drastically alters the growth time from cavity to cavity.
(3) Bubble activity, heat transfer, and fluid motion in the vicinity of an active site can substantially alter the growth pattern as well as the waiting period.
(4) Bubble shape continuously changes during the growth period.

Thus, correlations have been reported in the literature that include both the bubble diameter at departure and the bubble release frequency. One of the most comprehensive correlations of this type is given by Malenkov.[23] According to this correlation, product of bubble release frequency and diameter at departure are correlated as

$$fD_d = \frac{V_d}{\pi\left(1 - \dfrac{1}{1 + V_d\rho_G h_{LG}/q}\right)} \tag{16}$$

where

$$V_d = \left[\frac{D_d g(\rho_L - \rho_G)}{2(\rho_L + \rho_G)} + \frac{2\sigma}{D_d(\rho_L + \rho_G)}\right]^{1/2} \tag{17}$$

Bubble site density

As wall superheat or heat flux is increased, the number density of sites that become active increases. Gaertner and Westwater,[24] using a novel technique in which nickel from nickel salts dissolved in water was deposited on the heater surface, obtained the number density of active nucleation sites as

$$N_a \sim q^{2.1} \tag{18}$$

Hsu and Graham[7] have presented a summary of the earlier observations of several investigators with respect to dependence of site density on wall heat flux. Figure 1 shows the active nucleation site density data of Gaertner and Westwater[24] along with the data of Sultan and Judd.[25] Both sets of data were taken with water boiling at 1 atm on horizontal copper surfaces.

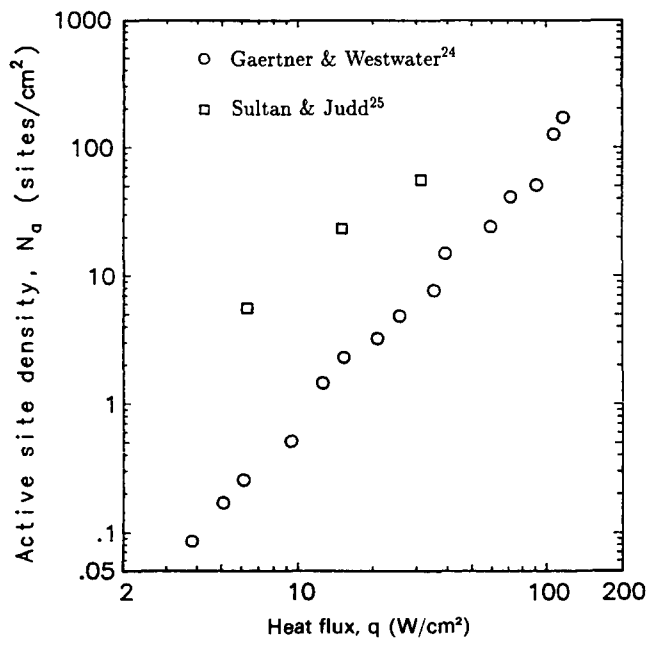

Figure 1 Comparison of cumulative nucleation site density observed by Gaertner and Westwater[24] and Sultan and Judd[25]

The data of Sultan and Judd show a weaker dependence on heat flux than the data of Gaertner and Westwater. However, the number of active sites in Sultan and Judd's experiments is several times higher than that reported by Gaertner and Westwater. It is found that the exponent on q generally varies between 1 and 2. The proportionality constant and the magnitude of the exponent depend on several parameters such as surface wettability, surface preparation procedure, and liquid properties and experimental conditions. Cornwell and Brown[26] made a systematic study of active nucleation sites on copper surfaces during boiling of water at 1 atm. Their study was limited to low heat fluxes, and the surface condition ranged from a smooth to a scratched rough surface. From their work, it was concluded that the active site density varied with wall superheat as

$$N_a \sim \Delta T^{4.5} \tag{19}$$

The proportionality constant in Equation 19 increased with surface roughness but the exponent on ΔT was independent of roughness. From an electron microscope measurement of cavity size distribution, they observed that the number density of cavities, N_s, on the surface was related to cavity size such that

$$N_s \sim \frac{1}{D_c^2} \tag{20}$$

By assuming that only conical cavities existed on the surface and that a minimum volume of trapped gas was needed for nucleation, they justified the observed functional dependence of active site density on wall superheat.

Singh et al.[27] compared nucleation behavior of water with organic liquids on four surfaces of different roughness. It was concluded that for a given boiling heat flux, the ratio of surface superheats required for two fluids remained constant and was unaffected by the value of surface roughness. They correlated the active nucleation site density, N_a, in the isolated bubble regime with

$$D_c = \frac{4\sigma T_{sat}}{\rho_G h_{LG}\,\Delta T} \tag{21}$$

The exponent on D_c or (ΔT^{-1}) was found to increase slightly with surface roughness. However, the proportionality constant increased significantly as the surface became rougher. Kocamustafaogullari and Ishii[28] have correlated the cumulative nucleation site density reported by various investigators for water boiling on a variety of surfaces at pressures varying from 1–198 atm as

$$N_a^* = [D_c^{*-4.4} F(\rho^*)]^{1/4.4} \tag{22}$$

where

$$N_a^* = N_a D_d^2; \qquad D_c^* = D_c/D_d \tag{23}$$

and

$$F(\rho^*) = 2.157 \times 10^{-7}\rho^{*-3.2}(1 + 0.0049\rho^*)^{4.13} \tag{24}$$

In the above equations, D_d is the bubble diameter at departure and is obtained by multiplying Equation 10 of Fritz[16] by $0.0012(\rho^*)^{0.9}$. The parameters ρ^* and D_c are defined as

$$\rho^* = \frac{(\rho_L - \rho_G)}{\rho_G} \tag{25}$$

$$D_c = 4\sigma[1 + (\rho_L/\rho_G)]/P_L \cdot \{\exp[h_{LG}(T_G - T_{sat})/(R_G T_G T_{sat})] - 1\} \tag{26}$$

In Equation 26, T_G is the temperature of vapor and P_L is the liquid pressure. At moderate pressures Equation 26 reduces to Equation 4 evaluated at low heat fluxes. For certain data an

order of magnitude deviation in the observed active site density was observed with respect to the correlation. One reason for the scatter may be that the correlation does not take into account the surface wettability and the surface roughness.

Mikic and Rohsenow[11] have proposed that on commercial surfaces the cumulative number of active sites per unit area can be assumed to vary in partial nucleate boiling as

$$N_a \sim \left(\frac{D_s}{D_c}\right)^m \tag{27}$$

where D_s is the diameter of the largest active cavity present on the surface and m is an empirical constant. The size, D_c, of a cavity that nucleates at a wall superheat ΔT is obtained from Equation 4. Bier et al.,[29] on the other hand, have deduced an expression for active site density from heat transfer data as

$$\ln N_a = \ln N_{max}\left[1 - \left(\frac{D_c}{D_s}\right)^m\right] \tag{28}$$

In Equation 28, N_{max} is the maximum value of N_a, which occurs at $D_c = 0$. The value of m was found to depend on the manner in which a surface was prepared. With Freon 115 or Freon 11 boiling on a chemically etched copper surface and on a turned surface, values of 0.42 and 0.26, respectively, were noted for m. In the heat transfer experiments, the reduced pressure was varied from 0.0037 to 0.9. It was found that to correlate the data at low and high saturation pressures some changes in the functional form of Equation 28 were necessary.

The studies on nucleation site density as described previously can be divided into two groups. In the first group are the studies in which the density of active nucleation sites as a function of wall superheat or heat flux has been obtained from experiments. In the second set of studies, the functional dependence of site density on wall superheat has been obtained by matching model predictions of heat flux with the data or vice versa. With the exception of Cornwell and Brown,[26] no attempt has been made in these studies to relate the cavities that exist on the surface to those that actually nucleate. Though Cornwell and Brown tried to determine the functional dependence of cumulative site density from the local distribution of cavities that exist on the surface, the attempt was qualitative in nature. Also, no attention was given to the surface wettability and shape of the cavities. More recently Yang and Kim[30] have made the first quantitative attempt to predict the active nucleation sites from a knowledge of the size and cone angle distribution of cavities that actually are present on the surface. Using a scanning electron microscope and a differential interference contrast microscope, Yang and Kim obtained the cavity probability density function in terms of the cavity diameter and cone angle. For cavities with mouth diameters varying from 0.65–6.2 μm, the cavity size distribution was found to fit a Poisson distribution.

$$f(D_c) = \lambda e^{-\lambda D_c/2} \tag{29}$$

whereas a normal distribution was used for half cone angle β,

$$f(\beta) = ((2\pi)^{1/2}s)^{-1} \exp[-(\beta - \bar{\beta})^2/(2s^2)] \tag{30}$$

In Equations 29 and 30, λ and s are statistical parameters and $\bar{\beta}$ is the mean value of the half cone angle. To determine the number of cavities that will trap gas or vapor and will eventually become nucleation sites, they used the criterion developed by Bankoff.[4] According to this criterion, the cavities will trap gas or vapor only if

$$\phi > 2\beta \tag{31}$$

Thus, combining Equations 29, 30, and 31, the cumulative density of active nucleation sites was expressed as

$$N_a = \bar{N}_s \int_0^{\phi/2} ((2\pi)^{1/2}s)^{-1} \exp[-(\beta - \bar{\beta}^2)/(2s^2)]\, d\beta \cdot \int_{D_c}^{D_s} \lambda e^{-\lambda D_c/2} dD_c \tag{32}$$

In the above equation, $\bar{N}_s$ is the average density of cavities present on the surface and D_s is the diameter of the largest cavity present on the surface and is obtained from statistical considerations. The magnitude of these parameters depends on the heater material and on the procedure used to prepare the surface. The predicted active nucleation site density was found to compare well with the data obtained at very low wall superheats. Though the scope of the study was limited, it represents a correct approach to a very difficult problem. The use by Yang and Kim of a Poisson distribution function for the cavities that exist on the surface after polishing is consistent with Gaertner's[31] observation that active nucleation sites were randomly located and could be represented by a Poisson distribution. However, transformation from the size distribution of cavities present on the surface to the density of sites that become active may be affected by several other parameters not included in the analysis of Yang and Kim.

By comparing gas and vapor bubble nucleation behavior, Eddington et al.[32] concluded that the number of active nucleation sites in boiling was much smaller than that in gas diffusion. The cause of this difference was thought to be the thermal interference between sites. From subcooled flow boiling experiments, Eddington and Kenning[33] have provided evidence that thermal interference inhibits nucleation within a region one diameter around an active site. This behavior in turn may distort random distribution of sites. Sultan and Judd[34] studied the bubble growth pattern at neighboring sites during nucleate pool boiling of water on a copper surface. They found that elapsed time between the start of bubble growth at two neighboring active sites increased as the distance separating the two sites increased. It was proposed that thermal diffusion in the substrate in the immediate vicinity of the boiling surface may be responsible for this behavior. Their work suggested that some relation may exist between distribution of active nucleation sites and bubble nucleation phenomenon.

Judd[35] in his summary of the results of nucleation site interactions notes that for dimensionless separation distances of $0.5 < S/D_d < 1$ between nucleation sites, the formation of a bubble at the initiating site promotes the formation of bubbles at the adjacent sites (site seeding). For separation distances $1 < S/D_d < 3$, formation of a bubble at the initiating site inhibits the formation of bubbles at the adjacent site (deactivation of sites). However, these observations are subjective to the number density of active sites. A detailed discussion of site interactions has also been given by Fujita[3] in his review article.

Heat transfer mechanisms

In the literature four mechanisms have been identified that contribute to total boiling heat flux under pool boiling conditions. These are transient conduction at the area of influence of a bubble growing on a nucleation site; evaporation (a fraction of which may be included in the transient conduction) at the vapor–liquid interface; enhanced natural convection on the region in the immediate vicinity of a growing bubble; and natural convection over the area that has no active nucleation sites and is totally free of the influence of the former three mechanisms. However, the importance of these mechanisms depends strongly on the magnitude of the wall superheat and other system variables such as heater geometry, orientation with respect to gravitational acceleration, magnitude of gravitational acceleration, etc.

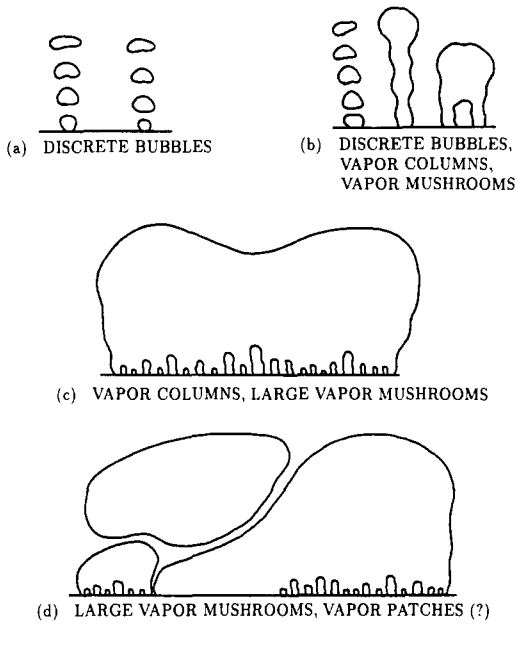

a. Discrete bubble region
b. First transition
c. Vapor mushroom region
d. Second transition region

Figure 2 Gaertner's[36] identification of vapor structures in nucleate boiling

From his now classical photographic study of pool boiling on a horizontal surface, Gaertner[36] identified several nucleate boiling regimes with different vapor structures. Figure 2 shows these vapor structures. After inception, discrete bubbles are released from randomly located active sites. All of the four mechanisms identified previously play a role in this region of partial nucleate boiling. Gaertner identified the transition (first transition) from isolated bubbles to fully developed nucleate boiling to occur when bubbles at a given site began to merge in the vertical direction. As a result of the merger of bubbles in the vertical direction, vapor appeared to leave the heater in the form of jets. This condition of formation of jets also approximately coincided with the merger of vapor bubbles at the neighboring sites. Thus, the vapor structure on the surface appeared like mushrooms with several stems. Figure 2b shows the structure that may exist on the surface at transition from partial to fully developed nucleate boiling. From Gaertner and Westwater's[24] study of nucleation site density, Zuber[37] concluded that transition from isolated bubbles to vapor columns and mushrooms occurred when the mean distance between neighboring sites became less than two bubble diameters. Moissis and Berenson[38] obtained a semitheoretical expression for Gaertner's first transition as

$$q = 0.11\sqrt{\phi}\,\rho_G h_{LG}\left[\frac{\sigma g}{(\rho_L - \rho_G)}\right]^{1/4} \tag{33}$$

where ϕ is the contact angle in degrees. Gaertner[36] observed that on heater areas over which vapor columns and vapor mushrooms were present, evaporation at the vapor–liquid interface of the vapor stems implanted in the thermal layer was the main mechanism of heat transfer.

At heat fluxes well above the heat flux at first transition, all of the heater area was covered with large vapor mushrooms. Heat was transferred by phase change at the vapor–liquid interface of the stems and also by evaporation at the base of the mushroom. At a heat flux of about 45 percent of his observed maximum heat flux, Gaertner identified a second transition. This transition corresponded to a rather large reduction in the slope of the nucleate boiling curve. Gaertner postulated that at these heat fluxes some vapor stems merged to form dry patches. A reduction in the slope of the q *versus* ΔT curve occurred because of a reduction in the number of vapor columns feeding a mushroom. It should be mentioned here that post second transition heat fluxes reported by Gaertner are much higher than the commonly accepted value of maximum heat flux for water boiling on a flat plate. Also, weak dependence on wall superheat of post second transition nucleate boiling heat fluxes on smooth surfaces has not been reproduced in the literature. Hence, this post second transition region should be treated with some skepticism.

The effect of orientation of a surface on the relative importance of the various mechanisms of boiling heat transfer can be seen from the data of Nishikawa et al.[39] plotted in Figure 3. The data were taken on a polished copper plate oriented at different angles, θ, to the horizontal. Saturated water at 1 atm was used as the test liquid. The data plotted in Figure 3 clearly show that in partial nucleate boiling there is a strong effect of orientation of plate with respect to gravitational acceleration. However, in fully developed nucleate boiling (the dotted line in the figure corresponds to prediction from Equation 33 with $\phi = 90°$), no such effect is discernible. The contributions of transient conduction and enhanced natural convection are affected by bubble dynamics, which in turn depends on the magnitude and direction of components of gravitational acceleration. The nondependence of fully developed nucleate boiling (post first transition) heat fluxes on plate orientation suggests that the mechanisms (transient conduction and enhanced convection) that are associated with bubble movement are of little consequence. The contribution of natural convection is generally small. Therefore, in fully developed nucleate boiling, evaporation appears to be the most dominant mode of heat transfer. This is consistent with the observations of Gaertner as discussed earlier.

Partial nucleate boiling

In the isolated bubble regime, transient conduction into liquid adjacent to the wall is probably the most important mechanism for heat removal from the wall. After bubble inception, the superheated liquid layer is pushed outward and mixes with the bulk liquid. The bubble acts like a pump in removing hot liquid from the surface and replacing it with cold liquid. This mechanism was originally proposed by Forster and Greif.[40] Mikic and Rohsenow[11] were the first to formalize the derivation of the functional dependence of partial nucleate boiling heat flux on wall superheat. Assuming that the contribution of evaporation to total heat removal rate was small they obtained an expression for the partial nucleate boiling heat flux as

$$q = \frac{K^2}{2}\sqrt{\pi(k\rho c_p)_L f}\,D_d^2 N_a\,\Delta T + \left(1 - \frac{K}{4}N_a \pi D_d^2\right)h_{nc}\,\Delta T \tag{34}$$

In Equation 34, the parameter K is reflective of the area of influence of a bubble, and a value of 2 was assigned to it. The site density N_a was obtained from Equation 27 whereas dependence on wall superheat ΔT of the size, D_c, of a nucleating cavity was obtained from Equation 4. For the bubble diameter at departure, D_d, Equations 11 or 12 were used. The product of bubble departure diameter and frequency, f, were obtained from the following correlation:

$$fD_d = 0.6\left[\frac{\sigma g(\rho_L - \rho_G)}{\rho_L^2}\right]^{1/4} \tag{35}$$

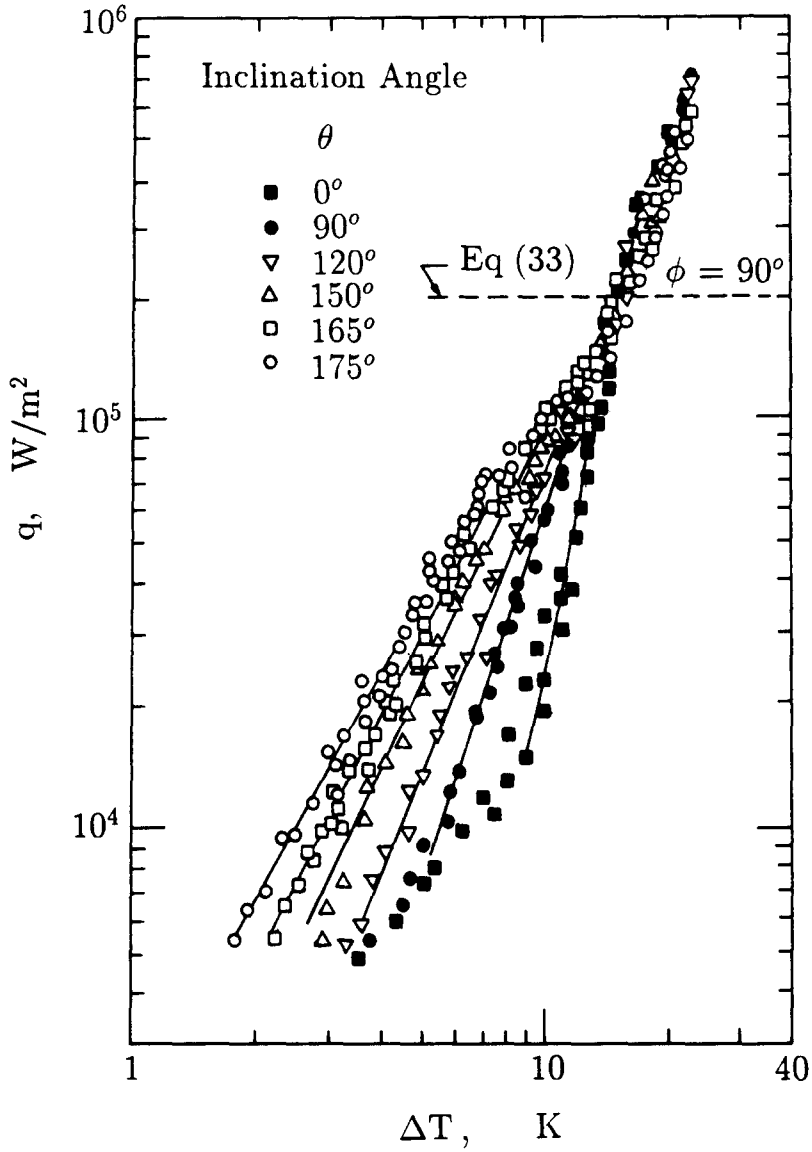

Figure 3 Nucleate boiling data of Nishikawa et al.[39] on plates oriented at different angles to the horizontal

For the natural convection heat transfer coefficient any of the correlations available in the literature could be used. It has been noted by Rohsenow[41] that predictions from Equation 34 show a better agreement with data when observed values for D_d and f rather than correlations are used. Equation 34 did yield the experimentally observed dependence of q on ΔT. It should be noted that a quantitative prediction from Equation 34 of dependence of heat flux on wall superheat requires a knowledge of several empirical constants. Though Equation 34 was derived for partial nucleate boiling, it has been suggested that Equation 34 could be extrapolated to fully developed nucleate boiling.

Judd and Hwang[42] employed an approach similar to that of Mikic and Rohsenow but included micro/macrolayer evaporation at the base of the bubble as well. Thus, a third term for microlayer contribution was added to the right-hand side of Equation 34 as

$$q_e = v_e N_a \rho_L h_{LG} f$$

where v_e is the volume of the micro/macrolayer associated with each bubble. Using the microlayer thickness measured from experiments in which dichloromethane was boiled on a glass surface, and assuming that parameter K in Equation 34 had a value of $\sqrt{1.8}$, they were able to match the predictions with the data. Experimentally measured values of active nucleation site density and bubble release frequency were also used in the model. Figure 4 shows their data and predictions. It is seen that at the maximum measured heat flux of about 6 W/cm^2 about a third of the energy is dissipated through evaporation at the bubble base.

More recently Paul and Abdel-Khalik[43] have made a detailed study of nucleate pool boiling of saturated water on a horizontal electrically heated platinum wire. From motion pictures, they determined the nucleation site density, bubble diameter at departure, and bubble release frequency. From this information, they were able to find the heat flux associated with phase change (evaporation). The natural convection contribution was determined from single phase convection data reported in the literature, whereas the contribution of enhanced convection was obtained by assuming that the bubbles created a flow normal to the heated surface. Figure 5 shows their evaluation of the contribution of various mechanisms to the total nucleate boiling

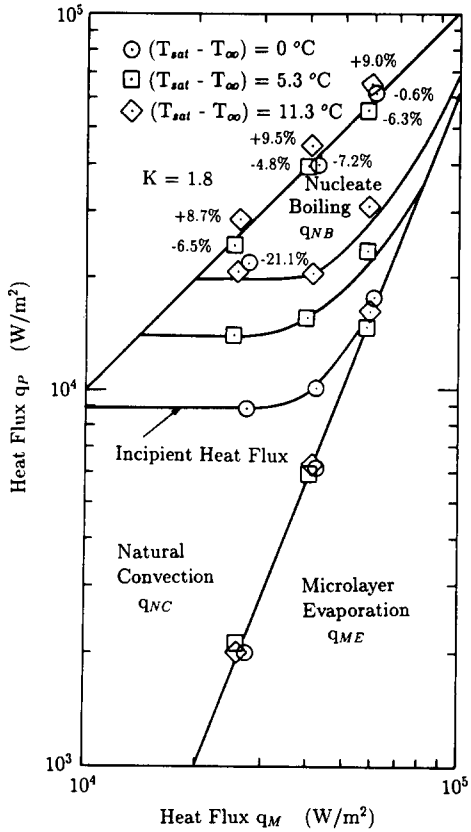

Figure 4 Relative contribution of various mechanisms to nucleate boiling heat flux[42]

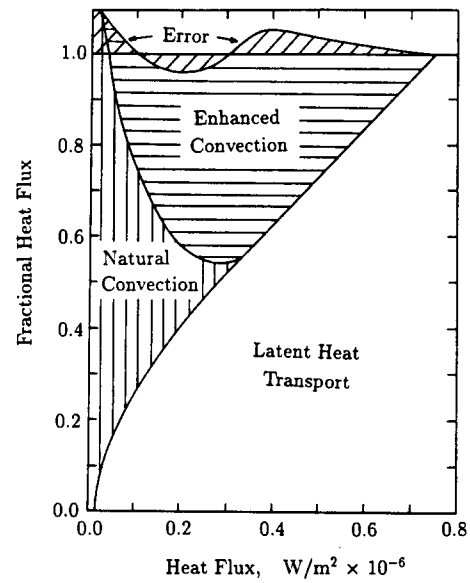

Figure 5 Relative contribution of various mechanisms to nucleate boiling heat flux as reported by Paul and Abdel-Khalik[43]

heat flux. From this figure it can be concluded that natural convection is the dominant mode of heat transfer at low heat fluxes. At intermediate and high heat fluxes phase change is a major contributor. Enhanced natural convection is important only in the intermediate region. The observed dominance of evaporation as heat flux increases is consistent with the observation of Judd and Hwang. This mode of heat transfer is not directly included in the model of Mikic and Rohsenow. Also, Mikic and Rohsenow and Judd and Hwang do not explicitly include enhanced convection, which has been found by Paul and Abdel-Khalik to play an important role.

In the isolated bubble regime, when the contribution of evaporation to the total heat flux is small, it appears that the approach used by Mikic and Rohsenow does have a mechanistic justification. The recent work of Paul and Abdel-Khalik does not support this observation, and it suggests that relative length scales for the heater and the bubble may represent an important consideration. Mikic and Rohsenow's model meets with moderate success when generalized correlations involving several empirical constants are used. However, as has been shown by Judd and Hwang[42] and Fath and Judd,[44] model predictions tend to compare very favorably with the data when micro/macrolayer evaporation is included in the model and information about site density, bubble diameter, and frequency is supplied from the same set of data.

Fully developed nucleate boiling

The studies of Judd and Hwang and Paul and Abdel-Khalik are in qualitative agreement with the observation of Gaertner[36] that after the first transition, evaporation is the dominant mode of heat transfer. According to Gaertner, most evaporation occurs at the periphery of vapor stems. Energy for the phase change is supplied by the superheated liquid layer in which the stems are implanted. Thus, the boiling heat flux can be calculated if the fractional area occupied by the stems and the thickness of the thermal layer are known. The heater area fraction occupied by stems (vapor) is equal to the product of the number density of stems and the area occupied by one stem. Gaertner and Westwater[24] found that the diameter of the stems decreased with heat flux as

$$D_o \sim (q)^{-1.43} \tag{36}$$

Gaertner[36] measured the temperature profiles in the thermal layer and made an assessment of the thickness of the thermal layer. He found that the temperature profile in the layer was exponential, and the conduction layer was much thinner than the overall thermal layer, which had a thickness equal to the height (thickness of the liquid layer between the heater surface and the base of the vapor mushroom) of the vapor stems. The height of the stems was about 60 percent of the diameter of the stems. Gaertner and Westwater[24] also inferred the magnitude of the wall void fraction from their stem diameter and number density data. The surface area covered by vapor was found to remain nearly constant in nucleate boiling. Though the data showed a large scatter, the void fractions varied between 4 and 15 percent.

Bobst and Colver[45] made a detailed measurement of temperature profiles in the thermal layer. From their work, it can be concluded that thermal layer thickness varies as ΔT^{-6}. This functional dependence is about the same as that given by Equation 36 of Gaertner and Westwarter if $q \sim \Delta T^4$ in fully developed nucleate boiling.

Iida and Kobayasi[46] were the first to make a direct quantitative determination of void fraction profiles near the heated surface. Using an electrical conductivity probe, they measured the void fraction during saturated boiling of water at 1 atm on the horizontal face of a 29-mm diameter copper cylinder. They found that in nucleate boiling maximum void fraction occurred at 0.3–1 mm from the surface. Since from the location of the maximum, the void fraction decreased both toward and away from the surface, a liquid-rich layer was identified to exist near the surface. The void fraction was found to increase with heat flux. This observation is in contradiction with the observation

of Gaertner and Westwater that the surface area covered by vapor is nearly independent of heat flux. Near the critical heat flux a maximum value as high as 90 percent for the void fraction was obtained. By correlating the spatial variation of void fraction with distance from the heater surface, Iida and Kobayasi deduced that the average and maximum thickness of the thermal layer decreased with heat flux. The functional dependence on heat flux and magnitude of film thickness were found to be about the same as the diameter of the vapor stems determined by Gaertner and Westwater.[24]

More recently, Liaw and Dhir[47] have measured the void fraction, α, profiles during saturated boiling of water on a vertical copper plate. They used a γ-densitometer to measure at high nucleate boiling heat fluxes the average void profiles across the plate cross section. The experimental results showed that for contact angles less than 90°, the maximum void fraction occurred at 1–1.5 mm away from the heater surface. However, for a contact angle of 90°, the void fraction in the vicinity of the surface did not vary with distance. The wall void fraction, the maximum void fraction, and the thickness of the void layer increased with wall heat flux. At a given heat flux, the wall void fraction decreased as the surface became more wettable. Figure 6 shows void profiles for a contact angle of 69°. In agreement with the results of Iida and Kobayasi, for moderately wetted surfaces, maximum void fractions approaching unity were observed near the peak nucleate boiling heat flux.

A recent attempt to deduce the thickness of the macrolayer from the bubble-release frequency is that of Bhat et al.[48] In the experiments they used an electrical resistance probe similar to that developed by Iida and Kobayasi. The definition used by Bhat et al. for the macrolayer is the same as that used by Gaertner[36] to define the liquid layer intervening the wall and the base of the mushroom. They correlated the macrolayer thickness, δ, as

$$\delta = 1.585 \times 10^5 q^{-1.527}\,(\mathrm{m}) \tag{37}$$

This functional dependence of δ on q is comparable to that observed by Gaertner and Westwater[24] and Iida and Kobayasi[46]; however, the magnitude of the thermal layer thickness is much smaller than that reported by Gaertner and Westwater and Iida and Kobayasi.

With the assumption that the vapor stem diameter is zero at the heater surface and increases linearly with distance from the surface, Bhat et al.[49] also developed a model to predict the thickness of the liquid layer between the heater surface and the vapor mushroom. However, in the model empirical expressions

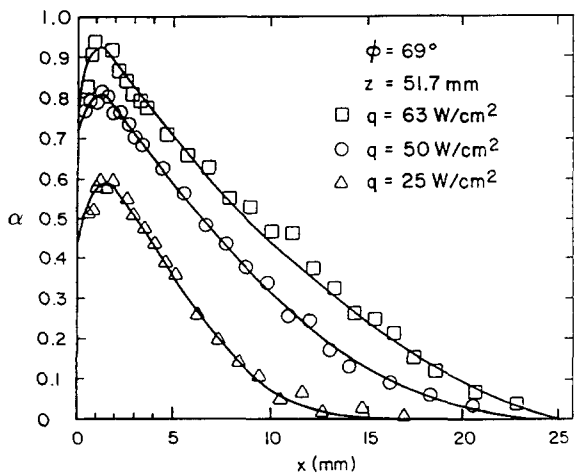

Figure 6 Void profiles adjacent to heated vertical plate

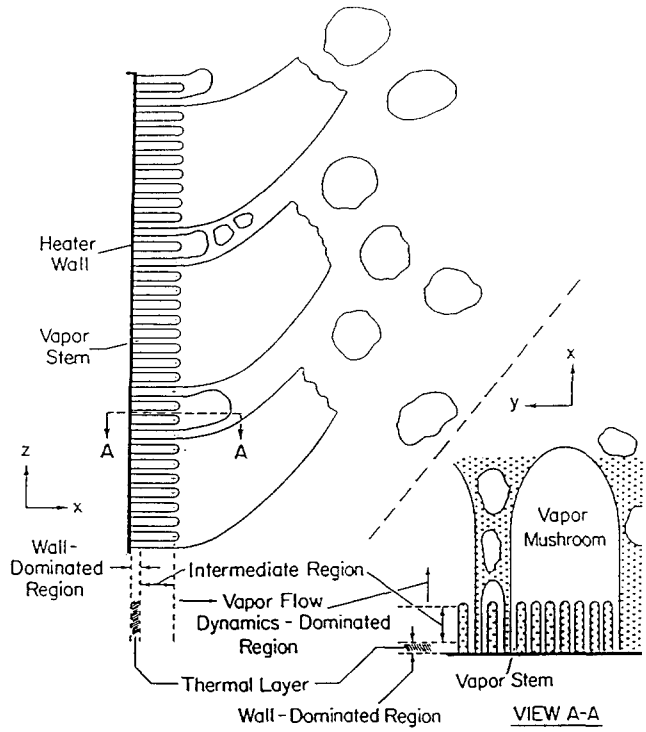

Figure 7 Liaw and Dhir's[47] conceptualization of the boiling process on a vertical surface

for site density, heat transfer coefficient, and product of bubble diameter at departure and frequency were used. These expressions implicitly related the thermal layer thickness with the heat flux. Bhat et al.[50] have also shown that at high heat fluxes, conduction across the liquid layer accounts for most of the heat transfer from the heater surface.

A time and area average model for fully developed nucleate boiling has been proposed by Dhir and Liaw.[51] The model employs vapor stems with a mushroom type of structure. Figure 7 shows their conceptualization of the boiling process on a vertical surface. They divided the vapor structure into three regions. The thermal layer containing vapor stems occupies the region immediately next to the wall. The thermal layer is strongly influenced by surface conditions and has a thickness of 10–100 μm. Vapor flow dynamics dominate the region beyond the location at which maximum void fraction occurs. The intermediate region lying between the outer edge of the thermal layer and the location at which maximum void fraction, α_{max}, occurs is influenced by both the wall and the vapor flow dynamics away from the wall. Concentrating only on the region in the immediate vicinity of the wall, it was assumed that vapor stems provided a stationary interface. Energy from the wall was conducted into the liquid micro/macrolayer and was used in evaporation at the stationary liquid–vapor interface. The heat transfer rate into the thermal layer and the temperature distribution in it were determined by solving a two-dimensional steady-state conduction equation in the liquid-occupied region. The heater surface area over which vapor stems existed was considered to be dry, and stems were assumed to locate on a square grid. Employing experimentally observed void fractions and assuming that

$$N_a \sim q^{1.5} \tag{38}$$

they were able to predict nucleate boiling heat fluxes observed during boiling of water on surfaces with different contact angles. The predictions were found to be in good agreement with the data. A comparison of the stem spacing and stem diameter

Table 1 Comparison of magnitudes of stem diameter and spacing with the data reported in the literature

	Dhir and Liaw[51] $\phi = 14°$			Gaertner and Westwater[24]		
ΔT, °C	q, W/cm²	D_o, m	L, m	q, W/cm²	D_o, m	L, m
25	61	1.18×10^{-3}	1.57×10^{-3}	44	9.50×10^{-4}	2.27×10^{-3}
30	103	9.11×10^{-4}	1.09×10^{-3}	96	2.48×10^{-4}	1.10×10^{-3}

predicted from the model is made in Table 1 with the data of Gaertner and Westwater.[24] The agreement is good except that the stem diameter observed at a wall superheat of 30°C is much smaller than that predicted from the model. In agreement with the observation of Bobst and Colver,[45] the calculated thermal layer thickness was reported to vary as ΔT^{-6}.

Peak heat flux

The peak heat flux sets the upper limit of fully developed nucleate boiling or the limit for the safe operation of a component. Kutateladze[52] and Zuber[37] were the first to provide a theoretical formulation for the peak heat flux. According to Zuber, the maximum heat flux condition occurs when the vapor velocity in the large jets leaving the heater surface reaches a critical value. At this value of the velocity, the vapor jets in a countercurrent flow situation become Helmholtz unstable and inhibit the outflow of vapor. The instability of the jets occurred away from the surface, and the surface conditions had little to do with the peak heat flux condition. Thus, Zuber laid the foundation of a theory that is now known as the hydrodynamic theory of boiling. By assuming that (1) all of the energy dissipated at the surface was used in phase change; (2) the vapor jets were located on a square grid with spacing equal to a Taylor wavelength; and (3) the jet diameter was equal to half of the Taylor wavelength, Zuber obtained an expression for the peak flux on an infinite horizontal plate as

$$q_{max_z} = \frac{\pi}{24}\rho_G h_{LG}\sqrt[4]{\frac{\sigma g(\rho_L - \rho_G)}{\rho_G^2}} \times \left\{\frac{\rho_L(16-\pi)}{\rho_L(16-\pi)+\rho_G\pi}\left(\frac{\rho_L+\rho_G}{\rho_L}\right)^{1/2}\right\} \quad (39)$$

Over the last three decades, Equation 39 has been found to be quite successful in predicting maximum heat fluxes on well-wetted large horizontal surfaces. As has been shown by Lienhard and Dhir,[53] Equation 39 predicts the flat plate data better if a constant of 0.15 instead of $\pi/24$ is used. The hydrodynamic analysis does yield such a constant if the Helmholtz unstable wavelength is taken to be equal to the most dominant Taylor wavelength. Kutateladze[52] also obtained an equation similar to Equation 39 from similitude analysis of the equations of momentum and energy.

The hydrodynamic theory as originally proposed by Zuber is limited to inviscid liquids and to infinite horizontal surfaces that are well wetted. The theory has been developed further by Leinhard and coworkers to account for the geometry and finite size of the heaters. The development of the theory as it applies to peak heat flux on cylinders was recently discussed by Lienhard[54] in his review article. According to the extended hydrodynamic theory, maximum heat flux on finite heaters can be written as

$$\frac{q_{max}}{q_{max_z}} = F(L') \quad (40)$$

where L' is the characteristic dimensionless length of the heater (e.g., radius of a cylinder, height of a ribbon, etc.) and is defined as $L' = L\sqrt{g(\rho_L - \rho_G)/\sigma}$. Figure 8 shows the hydrodynamic predictions of maximum heat flux for several geometries.

Dhir and Lienard[55] modified the hydrodynamic theory to account for the effect of liquid viscosity. Through analysis and experiments, it was shown that liquid viscosity enhanced the maximum heat flux.

Another limitation of the hydrodynamic theory is that it does not account for the effect of surface conditions. Despite some evidence in the literature that degree of wettability of the heater does affect the maximum heat flux, until recently little effort has been made to systematically quantify this effect. In 1965, Costello and Frea[56] found that on a 3-mm diameter half cylinder, the maximum heat flux with predeposited scale was reduced by a factor of about three when a drop of silastic was added to water. They also reported that the maximum heat flux on the same size half cylinder with predeposited scale was about 50 percent higher than that given by Equation 39. However, no such increase in the maximum heat flux with predeposited scale was observed on a 6-mm diameter half cylinder. The data for the peak heat flux on a 5.1-cm wide plate was also reported by Costello et al.[57] The maximum heat flux with tap water was about the same as that given by Equation 39; however, with distilled water the maximum heat flux dropped to about 40 percent of the value for tap water. Lienhard et al.[58] explained the latter observation from the hydrodynamic theory by accounting for the number of jets that could be accommodated by the heater. However, neither the difference in the magnitudes of the maximum heat fluxes with tap and distilled water nor the reduction in maximum heat flux with

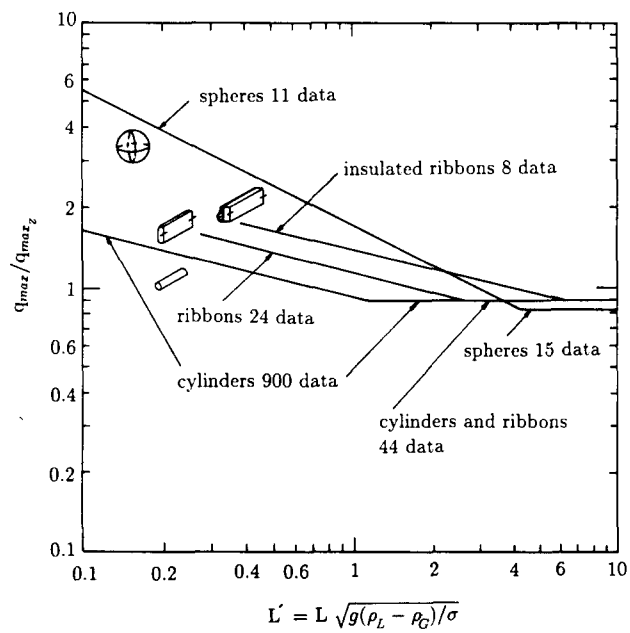

Figure 8 Prediction of maximum heat flux from the extended hydrodynamic theory[53]

addition of silastic nor the increase with predeposited scale could be explained from the hydrodynamic theory. Hasegawa et al.[59] have also reported a maximum heat flux of only 25 W/cm^2 during boiling of water on a partly wetted 2.9-cm diameter disk.

Very recently Liaw and Dhir[60] have studied systematically the effect of surface wettability on maximum heat flux. In their experiments saturated water at 1 atm was boiled on a vertical surface. The wettability of the surface was changed by controlling the degree of oxidation of the surface. A prescribed procedure was followed for oxidation, and the contact angle was used as a measure of the degree of wettability. The maximum heat flux data, which were obtained under steady-state heating of the surface, are plotted in Figure 9 as a function of contact angle. In this figure similar data of Hahne and Disselhorst[61] and Maracy and Winterton[62] are also plotted. From Figure 9, it is seen that maximum heat flux decreases as the contact angle increases. The data of Hahne and Disselhorst were obtained on horizontal cylinders of different materials, whereas the data of Maracy and Winterton were obtained on a horizontal surface. In comparison with the data of Liaw and Dhir and the data of Maracy and Winterton, the data of Hahne and Diesselhorst show a much stronger effect of contact angle. For a polished copper surface the contact angle, using the sessile drop method, was found by Liaw and Dhir[60] to be 90°. It is seen that maximum heat flux for this surface is about half that predicted from Equation 39. For contact angles less than about 20°, the observed maximum heat flux on the vertical surface is about the same as that obtained from the hydrodynamic theory. Based on this observation and from their model for fully developed nucleate boiling, Dhir and Liaw deduced that for partially wetted surfaces the rate of evaporation near the surface sets the upper limit of nucleate boiling heat flux, whereas for fully wetted surfaces the limit is probably set by the rate of vapor outflow. The solid line in Figure 9 shows the prediction from their thermal model.

The validity of using the Helmholtz instability of vapor jets in the hydrodynamic theory has recently been questioned by Haramura and Katto[63] on the ground that the vapor jets are too blunt to allow the development of the critical wave on the

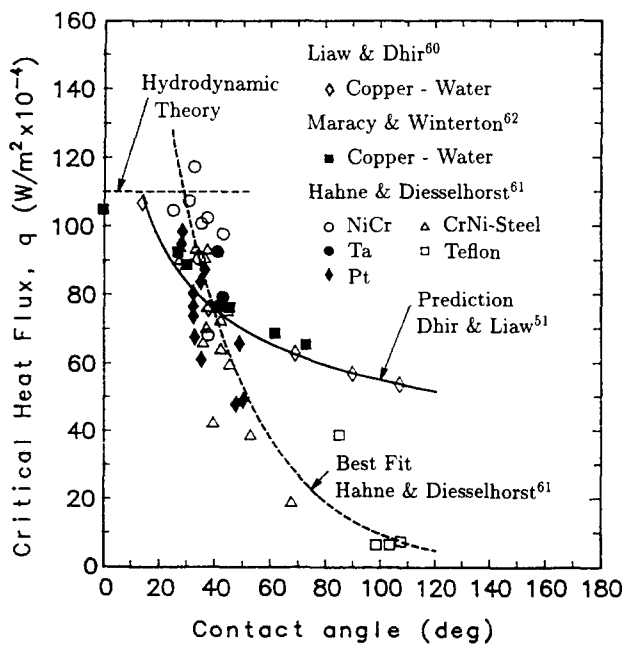

Figure 9 Dependence of maximum heat flux on contact angle

vapor–liquid interface. Instead, Haramura and Katto have proposed their own model. The cornerstone of their model is the suggestion made by Gaertner[36] that perhaps it is the Helmholtz instability of vapor stems that determines the maximum heat flux condition. Once the velocity through the stems was set by the Helmholtz instability, Haramura and Katto proposed that the maximum heat flux occurs when the liquid layer trapped between the heater surface and the base of the vapor mushroom dries out. The height of the vapor stem, which was assumed to be equal to one fourth the Helmholtz unstable wavelength, provided the length scale. The hovering period of a large vapor mass was used to determine the characteristic time. All of the pertinent variables were written in terms of the fractional area of the heater occupied by vapor stems, and this area fraction was determined by matching the predictions with Equation 39. As such the area ratio, A_G/A, was found to be a function of the vapor-to-liquid density ratio:

$$A_G/A = 0.0589(\rho_G/\rho_L)^{0.02} \tag{41}$$

According to this expression for water at 1 atm only about 1–1.5 percent of the heater area is covered by vapor stems. This appears to be an unrealistic value in light of the void data referred to earlier. As has been shown by Pasamehmetoglu and Nelson,[64] the area fraction obtained from the model of Haramura and Katto does not yield the macrolayer (liquid layer between the heater surface and the base of vapor mushroom) thickness that is consistent with the data of Bhat et al.[48] Haramura and Katto have also applied their model to other geometries such as a cylinder and to external flow boiling.

Transition boiling

Transition boiling is characterized by a reduction in surface heat flux with an increase in wall superheat. After Drew and Mueller[65] completed the boiling curve by obtaining data in transition boiling, the first well-documented and carefully conducted study on transition boiling is that of Berenson.[66] In Berenson's experiments n-pentane and carbon tetrachloride were boiled on a horizontal disk heated by condensation of steam underneath the disk. From the experiments in which heater surface conditions were also varied, Berenson[66] concluded the following:

(1) both liquid–solid and vapor–solid contacts occur in transition;
(2) all of the variables that affect the nucleate boiling also affect transition boiling;
(3) transition boiling is a combination of film and nucleate boiling alternately existing at a given location on the heated surface. The variation in heat flux with wall superheat is a result of change in the fraction of time each boiling mode is present at a given location.

As has been subsequently pointed out by Stephan[67] and Kovalev[68] and discussed by Hesse,[69] Berenson's apparatus allowed him access to only a few data points in transition boiling. Moreover, the accessible points from the nucleate boiling side were different from those obtained from the film boiling side. The accessibility issue has again recently been discussed by Ramilison and Lienhard[70] who recreated Berenson's experiment. Using maximum and minimum heat flux points as a guide, Berenson faired a curve through the limited data points available in transition boiling. He found that transition boiling heat fluxes on dirtier and more wettable surfaces were higher. Also, addition of oleic acid to pentane was found to push the transition boiling curve considerably higher. These observations

lead Berenson to propose that liquid–solid contacts existed in transition boiling. Berenson's conclusion was reconfirmed by Ramilison and Lienhard.

Transition boiling of F-114, F-12, and F-133 on a 14-mm outer diameter tube heated by forced flow of water through the tube has been reported by Hesse.[69] In his experiments Hesse satisfied the criterion proposed by Stephen[67] and was thus able to obtain a larger number of data points in transition boiling. All of the data reported by Hesse appear to be obtained while going from the nucleate to the film boiling side.

The reported studies on transition boiling are far fewer than those on nucleate and film boiling and consequently transition boiling is one of the least understood modes of boiling. One of the major reasons for the limited number of studies is the difficulty of carrying out steady-state transition boiling experiments. In temperature-controlled experiments, such as those reported by Berenson and Hesse, only limited data points are accessible because of the limitations imposed by the sum of resistances between the heat source and the heat sink. In heat flux controlled experiments it is the mismatch between the heat input and heat flux at the heated surface that causes the process to become time dependent.

To circumvent the latter difficulty, Peterson and Zaalouk[71] developed a feedback technique. This technique was later used by Sakurai and Shiotsu[72] to study transition boiling of water on horizontal wires. Sakurai and Shiotsu reported that a mixture of both film and nucleate boiling could be observed along the length of the wire. Thus, their data suffered from end effects. However, the data show the existence of hysteresis when transition boiling is accessed from nucleate or film boiling sides of the boiling curve. The subject of hysteresis in transition boiling is discussed later.

Very recently, Auracher[73] obtained steady-state transition boiling data for F-114 flowing in a 14-mm inside diameter nickel tube. The dither technique was used to carry out steady-state temperature-controlled experiments. It was concluded that in most of transition boiling, heat transfer over liquid-occupied regions of the heater dominates. As such, transition boiling was considered to be similar to nucleate boiling. The heat transfer coefficient in transition boiling was correlated as

$$h = C_2 q^{n_2} \tag{42}$$

In the narrow range of liquid mass velocities and qualities investigated, it was found that velocity and quality had little effect on the transition boiling heat fluxes. The observed similarly between nucleate and transition boiling is consistent with the approach taken by Dhir and Liaw[51] to describe transition boiling data on partially wetted surfaces. In their model, transition boiling was taken to be an extension of nucleate boiling.

With the presumption that a unique transition boiling curve exists, the earliest attempt to correlate transition boiling data was made by Kalinin et al.[74] Denoting the fraction of the heater surface in contact with liquid at a given instant by F_L, the transition boiling heat flux was written as

$$q = (F_L)q_L + (1 - F_L)q_G \tag{43}$$

In Equation 43, q_L is the time-averaged heat flux associated with liquid contacts and q_G is the heat flux over the surface covered with vapor. It should be noted here that this approach is different from Berenson's observation that transition boiling heat flux was determined by the fraction of time the liquid and the vapor contacted a particular heater location. Assuming that q_L and q_G were given by correlations for nucleate and film boiling, respectively, Kalinin et al. correlated the transition boiling data of cryogenics by evaluating, F_L, as

$$F_L = (1 - \overline{\Delta T})^7 \tag{44}$$

where $\overline{\Delta T}$ is defined as

$$\overline{\Delta T} = \frac{T - T_{max}}{T_{min} - T_{max}} \tag{45}$$

In Equation 45, T_{max} represents the heater temperature at which the maximum heat flux occurs and T_{min} is the minimum film boiling temperature. This formulation implies that F_L is unity at T_{max} and is zero at T_{min}. In reality, the surface is neither totally wet at T_{max} nor totally dry at T_{min}.

Bjornard and Griffith[75] replaced the nucleate and film boiling heat fluxes in Equation 43 with the maximum and minimum heat fluxes, respectively, to obtain an expression for transition boiling heat flux as

$$q = (F_L)q_{max} + (1 - F_L)q_{min} \tag{46}$$

where the fractional area, F_L, occupied by liquid was correlated as

$$F_L = \left[\frac{T_{min} - T}{T_{min} - T_{max}}\right]^2 \tag{47}$$

Because the minimum heat flux and the minimum wall temperature are known to be very sensitive to surface conditions and can vary over a wide range for a particular liquid–solid combination, the usefulness of an equation such as Equation 44 or 47 can be limited. It should be noted that Equation 44 and Equation 47 yield at a given wall temperature (except at T_{min} and T_{max}) values of F_L that differ widely.

Liaw and Dhir[60] have chosen to correlate transition boiling heat transfer coefficients rather than heat fluxes. Employing the concept that the wetted area of a heater is different from the area that is accessible to liquid, they wrote an expression for the transition boiling heat transfer coefficient as

$$\bar{h} = \beta_{horc}\bar{F}_L\bar{h}_L + \bar{h}_G(1 - \bar{F}_L\beta_{horc}) \tag{48}$$

In the above equation, $\bar{h}_L$ and $\bar{h}_G$ are the time-averaged heat transfer coefficients over wet and dry areas, respectively, $\bar{F}_L$ is the time-averaged fractional area of the heater accessible to liquid, and β_h or β_c is the factor representing the ratio of the fractional area of the heater that is wetted to the area that is accessible to the liquid. The parameter β_h is used when transition boiling is accessed from the nucleate boiling side, whereas β_c is for transition boiling established from the film boiling side. Figure 10 shows the dependence of β_h and β_c on the contact angle. These values were deduced from the transition boiling data for water obtained on a copper plate under quasi-static conditions. Liaw and Dhir proposed that even though the magnitudes of β_h and β_c depended on the manner in which transition boiling was accessed, the product $\bar{F}_L\bar{h}_L$ was a unique function of wall temperature for a particular liquid–solid

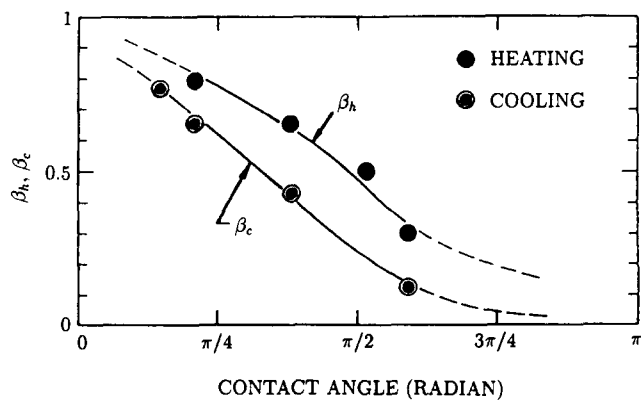

Figure 10 Dependence of parameters β_h and β_c on contact angle

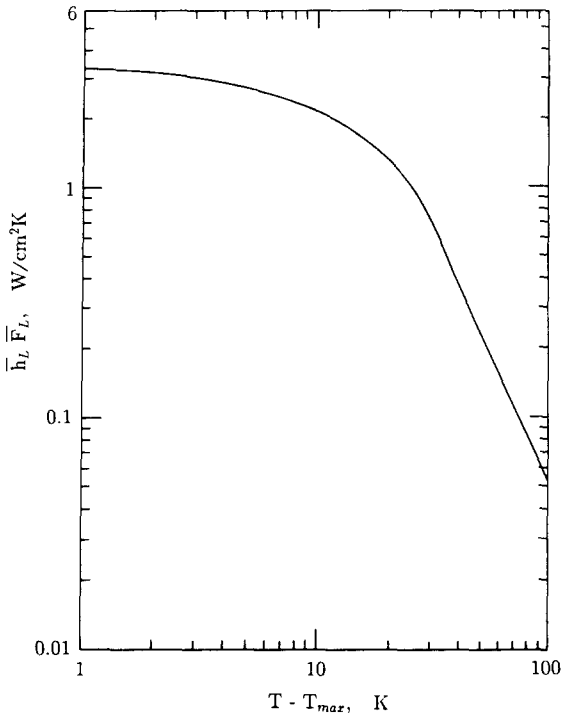

Figure 11 The variation of $\bar{F}_L\bar{h}_L$ with wall superheat in transition boiling

combination. Figure 11 shows a plot of $\bar{F}_L\bar{h}_L$ for saturated water at 1 atm. However, Liaw and Dhir were unable to obtain an explicit dependence of $\bar{F}_L$ on ΔT.

Hsu and Kim[76] have attempted to correlate transition boiling data by simulating the transition boiling with a Poisson distribution model. This simulation yields

$$\bar{N}_a A = f(\Delta T) \tag{49}$$

where $\bar{N}_a$ is the average number density of active sites and A is the cell area. The cell area was taken to be of the order of 10^{-6} m^2. The heat flux in transition boiling was written as

$$q = q_G + (q_L - q_G)F_L \tag{50}$$

The fractional area, F_L, occupied by liquid was obtained by considering the population density of bubbles. At maximum heat flux F_L had a value of 0.58. For transition boiling obtained from nucleate boiling side, Hsu and Kim[76] anchored the curve at q_{max} and for the transition boiling curve accessed from film boiling side, the minimum heat flux was used as an anchor point. This yielded the relationships

$$\frac{\Delta T}{\Delta T_{max}} = \frac{\bar{N}_a A}{1.41} \tag{51}$$

and

$$\frac{\Delta T}{\Delta T_{min}} = \frac{\bar{N}_a A}{(\bar{N}_a A)_{min}} \tag{52}$$

For curves anchored at the minimum heat flux $(\bar{N}_a A)_{min}$ was chosen to have a value of 7. The authors noted that their approach could include surface property and material effects when the number density of active sites was deduced by matching the predictions with the data.

An attempt to measure the duration of wet and dry contacts during transition boiling of water from a horizontal plate was made by Nishikawa et al.[77] They embedded a specially prepared thermocouple near the surface. The thermocouple was believed to have a response time of 10 μs. The frequency of contacts in transition boiling was found to be lower than that in nucleate boiling, but the contacts lasted for a longer period of time. By assuming that the rate of heat transfer during wet and dry contacts was given by nucleate and film boiling correlations, and that the wet area fraction was proportional to the fraction of the time a wet contact existed, Nishikawa et al. were able to calculate the transition boiling heat fluxes. Their calculated heat fluxes were, however, much lower than the observed heat fluxes. They argued that the thermal conditions near the probe were probably not representative of the average boiling conditions on the heater surface.

Ragheb and Cheng[78] also attempted to experimentally determine the wetted area during transition boiling. Normalizing the amplitude of the electric probe (zirconium wire) signal in transition boiling with that in the nucleate boiling and assuming that in the nucleate boiling all of the area was wetted, they determined the wet area fraction in transition boiling. They measured a wall void fraction of 0.15–0.2 at the maximum heat flux. The data of Ragheb and Cheng were found to compare well with the modification suggested by Tong and Young[79] to the correlation of Kalinin et al. Tong and Young had suggested that the wetted area fraction should be related to the transition and nucleate boiling heat fluxes as

$$F_L = \frac{q}{q_L} \tag{53}$$

Since the wetted area fraction, F_L, is influenced by liquid and surface conditions and is determined by first knowing q, the agreement between the data and Equation 43 is restricted to the experimental conditions employed in the study.

Wetted area fractions using an impedance probe have also been measured by Dhuga and Winterton[80,81] and Lee et al.[82] The data of Dhuga and Winterton were taken during transient transition boiling on the top surface of a 28-mm diameter aluminum cylinder. For saturated water a void fraction of about 0.1 is reported near the maximum heat flux. However, the void fraction data show strange behavior, in that at minimum heat flux only 80 percent of the surface area is covered with vapor. From the void and heat transfer data obtained with saturated water and methanol at 1 atm, the authors concluded that heat flux over the liquid-occupied region was not proportional to the wet fraction.

In the experiments by Lee et al.[82] liquid–solid contacts were measured with a fast response surface microthermocouple. The thermocouple was embedded in the center of a copper block that had a diameter of 101.6 mm. Transition boiling data for water were obtained in a quenching mode. Figure 12 shows the mean wet area fractions reported by Ragheb and Cheng,[78] Dunga and Winterton,[80] and Lee et al.[82] It is seen that while the data of Ragheb and Cheng and Lee et al. are comparable, the wet area fractions measured by Dhuga and Winterton generally tend to be high.

Most of the studies prior to 1974 were carried out under the belief that a unique transition boiling curve existed. Sakurai and Shiotsu[72] from their experiments on a horizontal wire documented the existence of hysteresis in transition boiling. Subsequently, Witte and Lienhard[83] suggested that thermal hysteresis observed by Sakurai and Shiotsu pointed to the existence of two transition boiling curves: the transitional film boiling curve and the transitional nucleate boiling curve. Referring to the experiments of Berenson[66] in which heat transfer had been observed to increase when oleic acid was added to the liquid, Witte and Lienhard argued that the increase in heat flux was the result of a shift from the transitional film boiling curve to the transitional nucleate boiling curve. Also, the jumps observed in transition boiling during quenching of

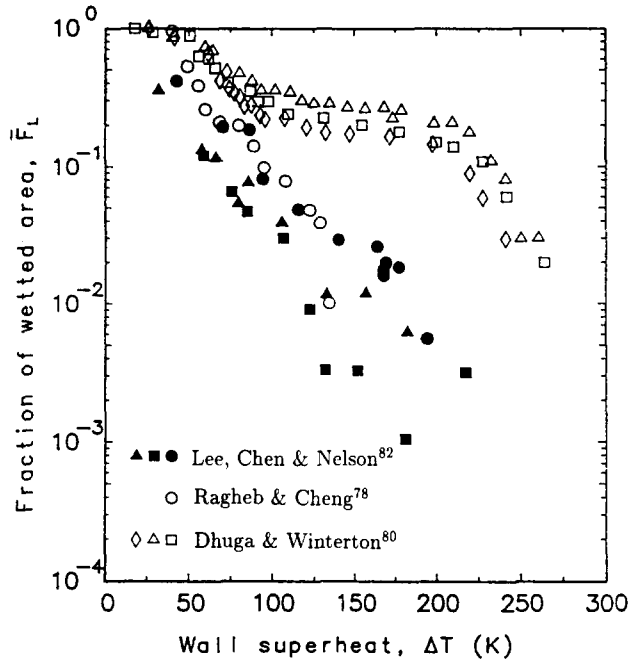

Figure 12 Comparison of wet area fractions measured in transition boiling by various investigators

small spheres were the result of a shift from the transitional film to transitional nucleate boiling curve. Bui and Dhir[84] studied transition boiling of water on a 6.3-cm wide and 10.3-cm high vertical surface that was machined from a large block of copper. They obtained transition boiling data both from the nucleate boiling and from the film boiling sides. On a smooth, clean surface they found two distinct transition boiling curves when transition boiling was approached from the nucleate and film boiling sides. Most of the transition boiling data were obtained under transient (quasi-static) conditions except the cooling data obtained near the minimum heat flux condition, which were obtained under a steady-state condition. Bui and Dhir tried to destabilize the transition boiling process by wiping the surface with a brush during the cooling mode. However, this procedure did not lead to a jump in the heat flux as has been hypothesized by Witte and Lienhard. The maximum heat fluxes obtained during cooling were generally smaller than those obtained under steady-state conditions.

Liaw and Dhir[60] have investigated the effect of surface wettability on hysteresis in transition boiling. The results of their experiments show that the difference between transition boiling heat fluxes obtained during heating and cooling of the surfaces diminishes as the surface becomes more wettable. No hysteresis was observed with F-113, which wets the surface well. Figure 13 shows the data for contact angles of 38° and 107°. The surface with a contact angle of 107° was obtained by depositing a thin coating of fluorosilicone sealant on the copper surface. It is noted from Figure 13 that hysteresis observed in transition boiling continues to persist in nucleate boiling. Figure 14 shows, as a function of contact angle, the maximum heat fluxes obtained in the transient cooling experiments. In this figure, the data obtained by Maracy and Winterton[62] on a horizontal disk are also plotted. The dotted line represents the best fit through the maximum heat flux data obtained in steady-state nucleate boiling experiments. The maximum heat fluxes obtained in the cooling experiments are seen to be always lower than those obtained in the heating experiments. The difference decreases as the contact angle becomes small. However, Maracy and Winterton reported that hysteresis persists even when the surface is totally wetted.

Variables affecting nucleate and transition boiling

Several experimental variables including heater surface characteristics can affect the boiling process. The influence on the boiling curve of a few of these variables was briefly discussed earlier. A summary of the role played by some of the important variables is given.

Surface finish

The data of Berenson[66] showed that the effect of increased surface roughness was to shift the nucleate boiling curve to the

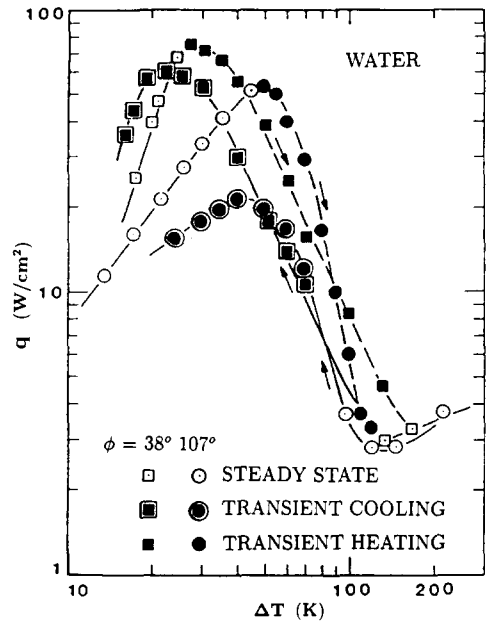

Figure 13 Transition boiling curves obtained on vertical surfaces having different contact angles

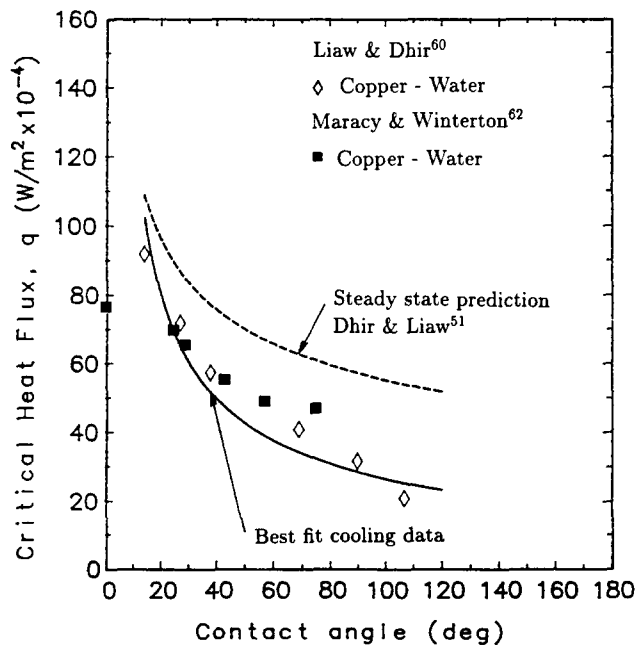

Figure 14 Dependence on contact angle of maximum heat fluxes obtained during transient cooling

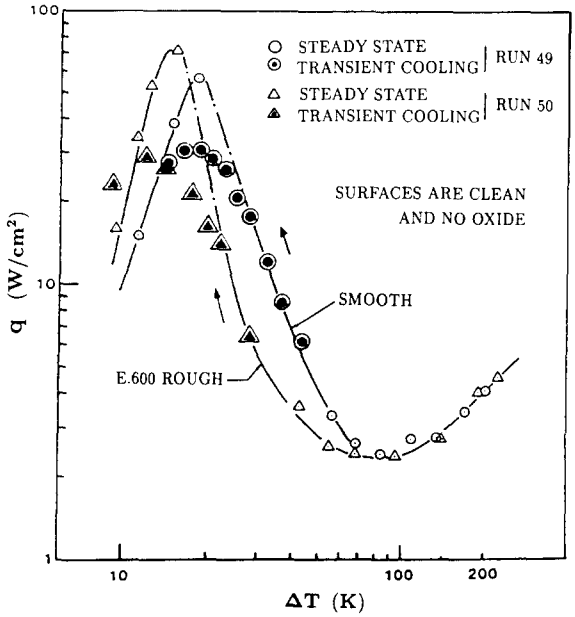

Figure 15 Effect of surface roughness on nucleate and transition boiling

left. This in turn corresponded to a higher heat flux at a given wall superheat for a rougher surface. The test liquids used in Berenson's experiments wetted the surface well, and it was noted that rougher surfaces also yielded slightly higher maximum heat fluxes. More recently, Bui and Dhir[84] obtained nucleate and transition boiling data for vertical copper surfaces of different finishes. Figure 15 shows their data for a clean mirror finish and an emery 600 finish surface. The behavior observed in nucleate boiling is similar to that reported by Berenson. However, during transient cooling the rough surface yields transition boiling heat fluxes that are lower than those observed on a smooth surface.

Generally, it is argued that on rough surfaces nucleation of larger cavities that require lower inception superheat leads to early onset of nucleate boiling. The rate at which new nucleation sites are added as wall superheat is increased is also higher for rough surfaces. Singh et al.[27] found that for nucleate boiling of water on a copper surface the exponent on ΔT in Equation 19 increased slightly with roughness. Shoukri and Judd[85] observed a trend opposite to that reported by Singh et al. An increase in the exponent results in a stronger dependence of wall heat flux on wall superheat. Bier et al.,[29] from their Freon data obtained on four surfaces prepared by following different procedures, concluded that a relation of the type

$$h \sim R_p^n \tag{54}$$

did not exist between heat transfer coefficient and roughness. In Equation 54, R_p is the surface roughness parameter. It should be mentioned here that three of the four surfaces used in the experiments had almost the same mean roughness but probably a different cavity size distribution because of the differences in procedures followed to prepare the surfaces. The work of Bier et al. suggests that it is important to distinguish between roughness and cavity size distribution, and any heat transfer model should account for both.

Surface wettability

With increase in surface wettability, the vapor trapping/retention capability of the cavities on a surface diminishes. This in turn delays the onset of nucleate boiling and shifts the boiling curve to the right. In liquids that wet the surface very well, inception of boiling at relatively high superheats can lead to hysteresis in the nucleate boiling curve. Figure 16 shows the nucleate boiling data of Liaw and Dhir[47] for different contact angles. In this figure fully developed nucleate boiling data of Nishikawa et al.[39] are also plotted. Two sets of data show a similar dependence of heat flux on wall superheat. However, data of Nishikawa et al.[31] appear to correspond to a contact angle of about 69°. It is seen that though with increase in the wettability of the surface the boiling curve shifts to the right, the functional dependence of heat flux on wall superheat remains nearly unchanged. As discussed earlier, the maximum heat flux on a partially wetted surface ($\phi = 90°$) is much smaller than that given by the hydrodynamic theory. It appears that for partially wetted surfaces, the maximum heat flux condition is determined by the rate at which vapor can be generated at the surface rather than by the rate at which vapor can be removed without any restriction.

In transition boiling, the magnitude of observed hysteresis between transient heating and cooling is affected by the surface wettability. Since the cavity shape and the contact angle affect the vapor/gas retention capability, any predictive model for density of active nucleation sites must rely on the information about the size distribution and the shape of the cavities that are present on the surface.

Surface contamination

Physicochemical changes of a boiling surface can take place in several ways: deposition of inert matter contained in the host liquid; slow chemical reaction of the surface with the gases dissolved in the liquid or with the vapor; and strong chemical reaction of the metal with the concentrated solutions of electrolytes. The latter two processes continued over a long period of time can lead to a loss of material or corrosion of the surface. Corrosion can also result from repeated collapse of

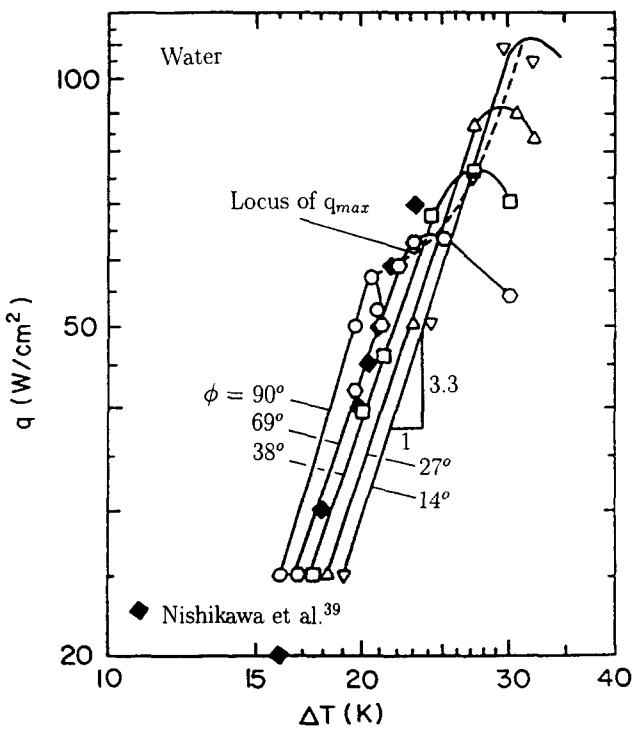

Figure 16 Effect of surface wettability on nucleate boiling heat fluxes

vapor bubbles subjected to subcooled liquid and collision of bubbles with the heated surface during flow boiling.

The presence of foreign material on the surfaces can affect the nucleation behavior of the surface by deactivating some cavities, by providing new nucleation sites, and by changing the wettability of the surface. As yet no basis exists for quantification of the effect of surface cleanliness on nucleate and transition boiling. Recently Bui and Dhir[84] obtained water data on clean and dirty surfaces. The dirty surfaces were obtained by prolonged nucleate boiling of water that had been exposed to the atmosphere. Over time the surface became contaminated with dirt particles contained in water. Various degrees of dirt deposits were obtained by varying the boiling time. Dirt deposits were found to have a small effect on the nucleate boiling curve. However, the maximum heat flux on the surface subjected to longest boiling period was about 25 percent higher than that on a clean surface. The difference between transition boiling data obtained during heating and cooling of the surface decreased as the surface became dirtier. This behavior is similar to that observed with change in wettability of the surface. For the surface subjected to the longest boiling time, the two transition boiling curves obtained during heating and cooling nearly overlapped.

The presence of oxygen in the host liquid leads to contamination of the surface via slow chemical reactions. The process, if continued over a long period, can lead to aging of the surface or a permanent change in the boiling characteristics of the surface. Metal ions from the pits or cavities on the heated surface or from the fittings can be dissolved in the host liquid. The metal ions combine with oxygen to form metal oxides that precipitate at the heated surface. Joudi and James[86] identified the precipitate in the form of small brown spots around the cavities or at the base of the bubbles where high heat and mass transfer gradients exist. The effect of contamination of the surface was to push the boiling curve to the right or to increase the wall superheat for a given heat flux. This effect is similar to that of improved wettability of the surface. Joudi and James found that after one or two runs with water, the stainless steel surface could be rejuvenated by boiling of refrigerant 113. Some of the variability in the data reported in the literature can be attributed to the aging of the surface.

Ross[87] in his review article on corrosion and heat transfer, reports results of long-term boiling (hundreds of hours) of water on iron, copper, and aluminium surfaces. It was found that mass loss rate increased with concentration of oxygen in water. At low heat fluxes, the mass loss rate was independent of heat flux, but at high heat fluxes a reduction in mass loss rate was observed as heat flux was increased. When sodium chloride (electrolyte) was dissolved in water, the mass loss rate curves showed a local minima with respect to nucleate boiling heat flux. At low heat fluxes, the mass loss rate decreased with heat flux but at high heat fluxes an opposite trend was observed. It was suggested that minima in mass loss rate may be due to competing effects of oxygen and chloride ions at the interface.

Heater geometry, size, material, and thickness

The boiling inception superheat and partial nucleate boiling heat fluxes can be strongly affected by convective flow patterns and bubble movement on and around the surface. The convective flow itself is influenced by the heater geometry, size, and to some extent by the size and shape of the container.

The data of Nishikawa et al.[39] plotted in Figure 3 clearly show the effect of the angle of inclination of the plate on the inception superheat and on the partial nucleate boiling heat fluxes. Surprisingly, the nucleate boiling heat transfer coefficient is higher when the surface is facing downward than when it is horizontal or vertical. The enhancement in heat transfer on downward-facing surfaces probably results from the disruption of the thermal layer caused by bubbles sliding along the wall. In fully developed nucleate boiling no such effect of angle of inclination is evident.

The earliest study of nucleate pool boiling heat transfer on horizontal cylinders is that of Lance and Myers,[88] whereas the most recent study is that of Cornwell and Einarsson.[89] Both pool and low flow velocity conditions during nucleate boiling heat transfer on a horizontal tube have been considered by Cornwell and Einarsson. Special care was taken in their experiments to minimize the effect of conduction in the circumferential direction. Figure 17 shows their data obtained with saturated Freon 113 at 1 atm. Under pool boiling conditions, the heat transfer coefficient is highest at the lower stagnation point and is lowest at the top. However, the heat transfer coefficient remains fairly constant over most of the periphery of the cylinder. The heat transfer coefficient profile observed during boiling is much flatter than would be expected under single phase natural convection conditions. At small imposed flow velocities, the location of maximum heat transfer coefficient shifts to the sides of the tube. It was suggested that sliding of the bubbles probably led to a higher heat transfer at the sides. Cornwell and Einarsson concluded that because of the sensitivity of the flow field to chamber geometry and the tube diameter and the dependence of the nucleate boiling process on surface conditions, it is extremely difficult to predict with any reasonable accuracy the nucleate boiling heat fluxes at low velocities and low superheats.

Though the data of Nishikawa et al.[39] show that fully developed nucleate boiling is not affected by the plate angle of inclination, the wealth of data reported in the literature show that the size and geometry of the heater do influence the maximum heat fluxes. From the hydrodynamic predictions plotted in Figure 8, it is noted that for $L' \leq 2$, heater size and geometry play a significant role. However, as the characteristic dimension of the heater becomes large, the effect of the size of the heater vanishes. A small effect of heater geometry does persist, however. Most of the data in the study of Lienhard and Dhir[53] were obtained under well-wetted surface conditions. For partially wetted surfaces not enough maximum heat flux data on heaters of different sizes and geometries are available to quantify the effect of these variables. From the data plotted in Figure 9 it can be inferred that partially wetted cylinders behave differently from a horizontal or a vertical plate. However, it should be mentioned that the data of Hahne and Diesselhorst were obtained on cylinders of different materials and therefore some uncertainty may exist with respect to the measured contact angles.

Heater geometry and size probably influence transition boiling as well. However, not enough data under well-defined heater surface conditions are available in the literature to make any conclusive statement.

In steady-state experiments, the heater material properties can play a role through such surface characteristics as cavity size distribution, cavity shape, and wettability. If the heaters are very thin, the thickness of the material has been shown to affect the maximum heat flux in a significant way. Houchin and Leinhard[90] and Tachibana et al.[91] found that on thin heaters maximum heat flux occurred prematurely. In both of these investigations the reduction in the maximum heat flux was correlated with the product of the thermal conductivity, specific heat, and thickness of the heater material. It was postulated that the hot spots under vapor bubbles or jets probably led to premature burnout. The data of Tachibana et al. also showed that in comparison to DC heating, the reduction in maximum heat flux in thin heaters was larger with AC heating.

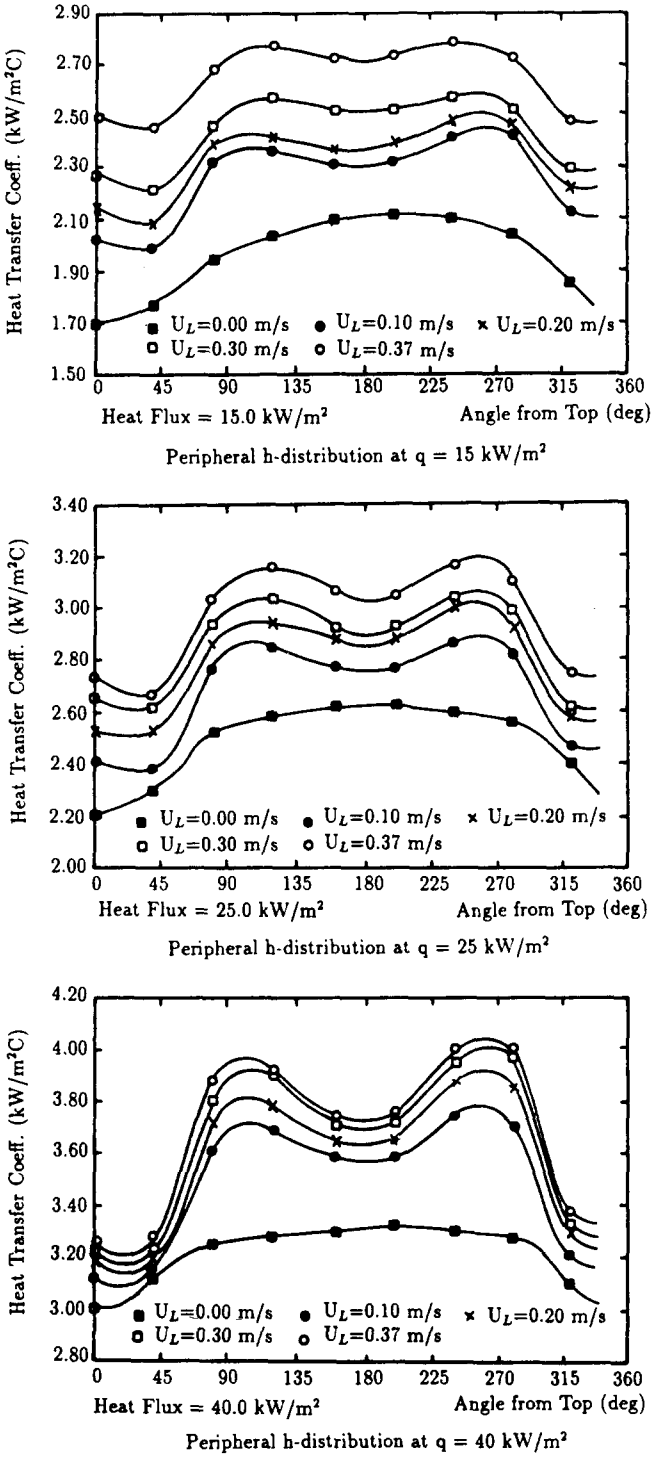

Figure 17 Circumferential variation of partial nucleate boiling heat fluxes on a cylinder[89]

System pressure

With an increase in system pressure, the incipience superheat decreases and the nucleate boiling curve is shifted to the left. The maximum heat flux initially increases with pressure, attains its highest value between reduced pressures of 0.3 and 0.4, and thereafter decreases with pressure. Fath and Judd[44] showed that Mikic and Rohsenow's[11] model for partial nucleate boiling, with the contribution of micro/macrolayer evaporation included in it, was also applicable at pressures lower than 1 atm. However, several of the parameters used in the model were determined from experiments that also provided heat transfer data. Gorenflo et al.[19] have correlated the nucleate boiling heat transfer coefficient data for Freon 12, Freon 22, and propane obtained at reduced pressures, P^*, up to 0.93 as

$$\frac{h}{h_0} = \left(\frac{q}{q_0}\right)^n \cdot F(P^*) \tag{54}$$

where

$$F(P^*) = 2.1P^{*0.27} + \left(4.4 + \frac{1.8}{1 - P^*}\right)P^* \tag{55}$$

and

$$n(P^*) = 0.9 - 0.3P^{*0.3} \tag{56}$$

The values of the reference heat transfer coefficient h_0 at the reference heat flux, $q_0 = 2 \times 10^4$ W/m² and the reference pressure, $P_0^* = 0.03$ for the three liquids are

	F-12	F-22	C_3H_8
h_0	2,300	2,200	2,100 W/m² K

Gorenflo et al. also extended the isolated bubble model of Mikic and Rohsenow to high heat fluxes, with the assumption that despite the overlapping of the areas of influence, the single bubble formulation remained unchanged. They also assumed that frequency of liquid replacement at dense bubble packings was higher than that for isolated bubbles. Up to reduced pressures of 0.8, the model predictions tended to show only qualitative agreement with the data. For well-wetted surfaces, Equation 39, based on the hydrodynamic theory, yields predictions for the maximum heat flux that are in good agreement with the data obtained over a wide range of pressures.

Gravity

The magnitude and direction of the gravitational acceleration with respect to the heater surface influence the convective hydrodynamic and thermal boundary layers and bubble trajectory. On a given surface the thermal layer thickness and the temperature profile in the thermal layer determine the inception superheat. In partial nucleate boiling, heat transfer by convection represents a major fraction of the total heat transfer rate. Thus, gravity plays an important role in this mode of boiling. Figure 18 shows the nucleate boiling data obtained at different magnitudes of acceleration. The data are for liquid nitrogen boiling at 1 atm, and as recently reported by Merte,[92] were obtained by Merte and coworkers in the early 1960s. The high gravity data were taken in a centrifuge, the near zero gravity data in a drop tower, and the data obtained on a downward-facing horizontal disk were considered to be -1 g data. All of the data were taken under transient boiling conditions. At low heat fluxes, the magnitude of gravity appears to affect the boiling curve. However, at high nucleate boiling heat fluxes no effect of gravity is evident. At low wall superheats, the heat fluxes associated with near zero g and -1 g are higher than those obtained when a large body force was present. On a downward-facing surface, the bubbles move along the surface and thereby enhance the heat removal rate by disruption of the thermal layer over a larger area. At zero gravity, the bubbles in these transient experiments probably persisted for a longer period and thereby enhanced the evaporative contribution to total heat transfer rate.

Reduced gravity nucleate boiling data of Zell et al.[93] are shown in Figure 19. These data were obtained with F-12 boiling at different pressures on a platinum wire. Reduced gravity conditions were created in parabolic flight of a C-135 airplane.

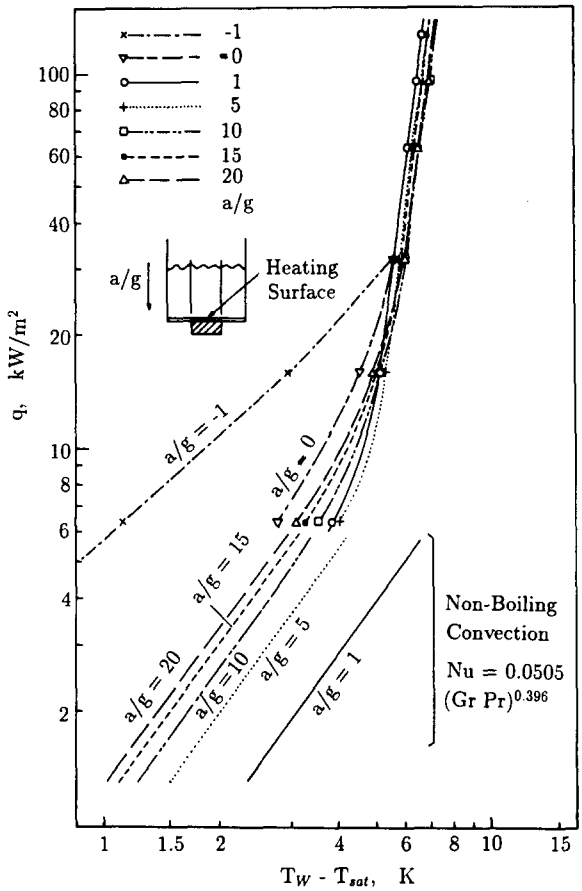

Figure 18 Effect of body force on nucleate boiling heat fluxes[92]

The various curves in Figure 19 correspond to the best fit through the data obtained at earth normal gravity. The symbols represent reduced gravity data. Almost no effect of gravity on heat transfer is noted even though at the microgravity condition bubbles were larger than those at earth normal gravity. The near zero gravity conditions were also found to have little effect on subcooled nucleate boiling.

According to the hydrodynamic theory, the maximum heat flux should vary with gravity as $\sqrt[4]{g}$. The high gravity centrifuge data do confirm this dependence. However, the drop tower data of Siegel and Usiskin[94] showed that the value of the exponent of gravity decreases as the magnitude of gravitational acceleration is reduced, and at very low gravity the maximum heat flux is independent of gravity. At present no rational basis exists to explain this behavior. At microgravity conditions many internal and external factors (e.g., thermocapillary forces, vibrations, etc.) can influence the process.

Mode of the experiments

The boiling curve can be affected by the manner in which the experiments are conducted—steady state or transient. Most of the discussion presented previously is that for a steady-state process. One of the earliest studies on transient nucleate boiling heat fluxes is that reported by Johnson.[95] In the experiments thin metallic ribbons submerged in water were heated electrically. The power to the heaters was increased exponentially. It was concluded that for exponential periods greater the 5 ms, the transient nucleate boiling process including incipience could be described by a steady-state process. However, the transient maximum heat fluxes exceeded the steady-state values. Subsequent studies of Sakurai and Shiotsu[96,97] on platinum wires submerged in a pool of water show that for exponential periods varying from 5 ms to 1 s, the incipience heat fluxes increase as the exponential time decreases. In nucleate boiling, the transient heat transfer coefficients were generally found to be lower than those obtained under steady-state conditions. The ratio of the transient and the steady-state heat fluxes depended on the magnitude of the heat flux, but values as low as 0.5 for this ratio were reported. For periods less than 100 ms, the transient maximum and DNB heat fluxes were found to increase as the exponential time decreased. The DNB heat flux was defined as the highest nucleate boiling heat flux at which a linear relationship between $\ln q$ and $\ln \Delta T$ ceased to exist. Figure 20 shows their data obtained at pressures ranging from 1–20 atm. Kozawa et al.[98] have also studied transient boiling from a 70-μm thick copper foil submerged in a pool of F-113. Their objective was

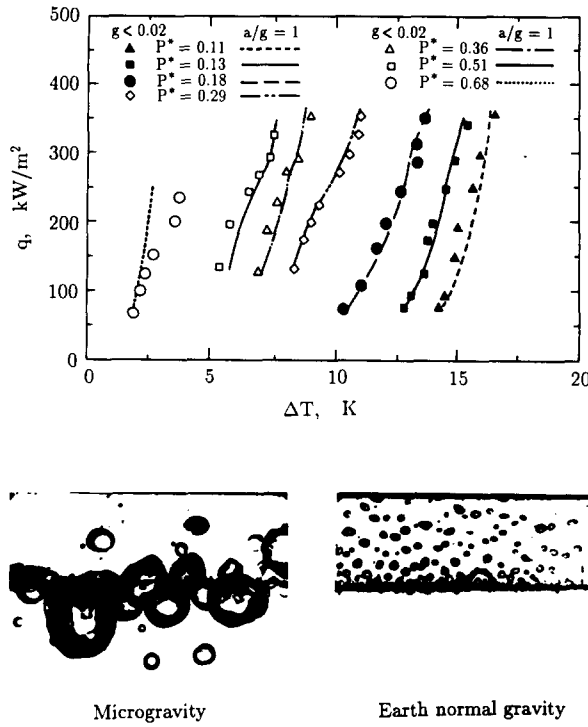

Figure 19 Comparison of pool boiling data obtained by Zell et al.[93] at earth normal gravity and at microgravity conditions

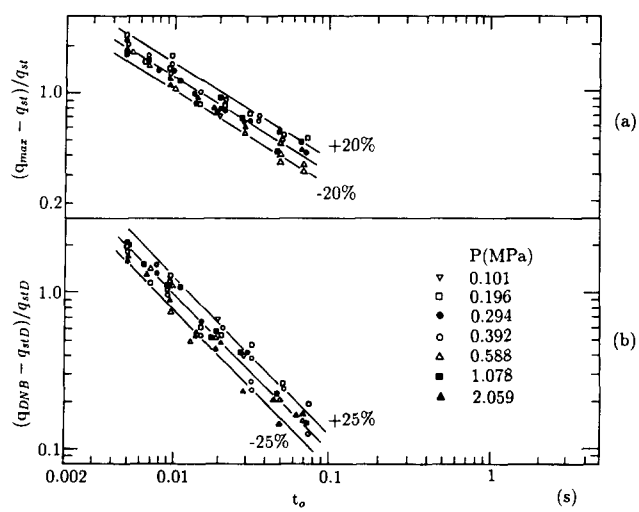

Figure 20 Effect of transient time on DNB heat flux[96,97]

to determine the magnitude of the wall superheat at the onset of transition boiling rather than the magnitude of the maximum heat flux. Stepwise heating was used and artificial pinholes were created on the surface to enhance nucleation site density and thereby the rate of heat transfer. An optimum pinhole density was found for enhancement of boiling heat transfer. The authors found that the presence of pinholes limited the temperature overshoot. The onset of boiling transition was not only affected by the magnitude of the heat flux but also by the wall superheat at boiling incipience.

Models for transient maximum heat fluxes have been proposed by Serizawa[99] and Pasamehmetoglu et al.[100] These models employ an accepted steady state critical heat flux model as a starting point. In the work of Pasamehmetoglu et al., the steady-state model of Haramura and Katto[63] was used while including the effect of time-dependent heat flux on the initial liquid layer thickness (hydrodynamic basis) and on the evaporation rate of the liquid layer. The conduction equation in the heater was also solved to relate the surface heat flux to the energy generation rate in the solid. The predictions from the model were reported to be in good agreement with the data. The hovering period of a bubble was an adjustable parameter in the model.

Quenching of a hot body in a saturated or a subcooled liquid has many industrial applications. To circumvent the difficulties associated with carrying out steady-state boiling experiments in certain geometries and to facilitate acquisition of data in transition boiling, quenching (transient cooling) has also been used as an experimental technique for carrying out boiling studies. In the quenching experiments the time-dependent temperature history in the solid is used to recover the surface heat flux. If quenching is used as an experimental technique, such questions arise as how well the transient boiling curves can be identified with a steady-state process, and what criterion or conditions need to be satisfied before quenching results can be considered to approach steady-state results? Bergles and Thompson[101] and Veres and Florschuetz[102] made the first two attempts to relate the transient boiling curves to the steady-state boiling curves. Bergles and Thompson reported that maximum heat fluxes in their transient and steady-state tests were about the same, while some differences existed in the steady and transient transition boiling data. However, Bergles and Thompson did not use the same heater geometry in the two tests. Veres and Florschuetz, by employing the same heater in the two types of tests, eliminated the heater geometry as a parameter. But they introduced another new variable in terms of induction heating that was used to carry out the steady-state experiments.

Peyayopanakul and Westwater[103] studied the boiling process during quenching by systemically varying the time needed to quench the heater surface. In the experiments, 5.08-cm diameter horizontal copper disks of thickness varying from 0.05–51 cm were used. Liquid nitrogen at 1 atm was used as the test liquid. Figure 21 shows the boiling curves obtained in their experiments. From the data the authors concluded that disk thickness had no effect on nucleate and transition boiling as long as the thickness was greater than 1.3 cm. For thinner test specimens, the boiling curves were generally shifted to the right. The maximum heat flux decreased with decreasing thickness when the disk was thinner than 2.5 cm. For thicknesses greater than 2.5 cm, the maximum heat flux was independent of thickness. It was noted that if the time to traverse the top 10 percent of the boiling curve was greater than 1 s, the boiling process could be called quasi-steady.

In a subsequent work, Lin and Westwater[104] investigated the effect of thermal properties of the solid on the boiling process during quenching. They noted that the required thickness of the test specimen for the process to be called quasi-steady was

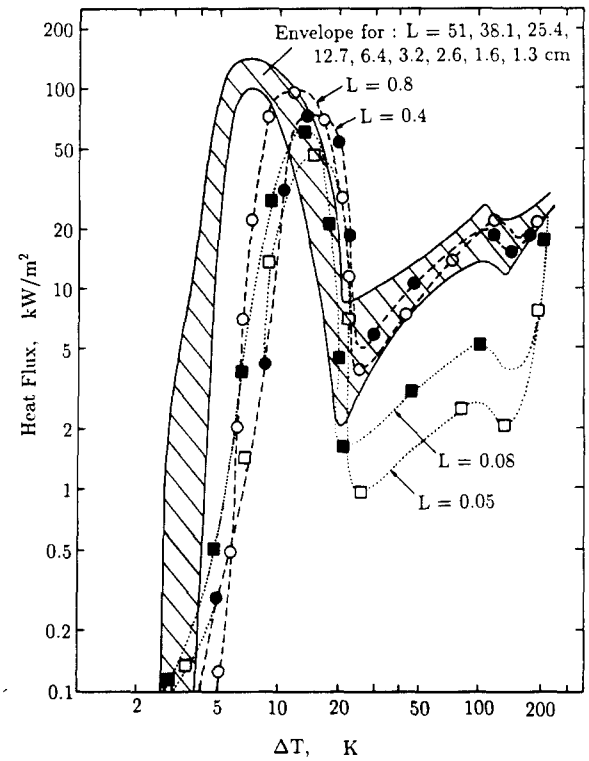

Figure 21 Transient pool boiling curves of nitrogen boiling on horizontal copper disks of different thickness[103]

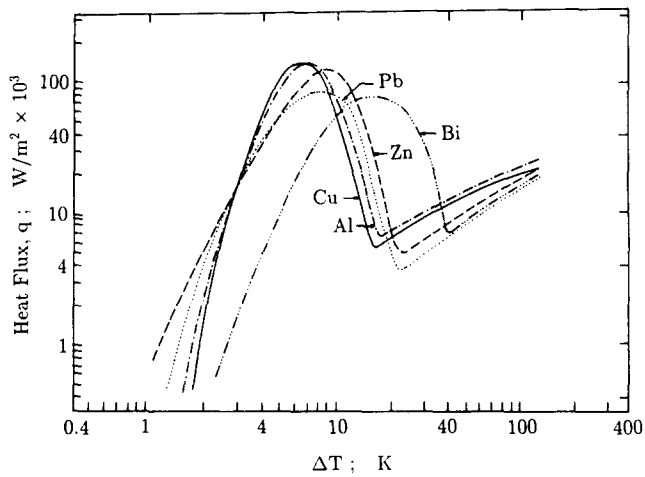

Figure 22 The effect of metal properties on boiling curves obtained during quenching[104]

different for each metal. Figure 22 shows their quasi-steady boiling curves for the five metals tested. Some effect of the specimen thermal properties on nucleate and transition boiling is evident. The quasi-steady maximum heat flux was correlated with the product of density, specific heat, and thermal conductivity. The effect of metal properties during quenching of spheres has been reported by Irving and Westwater.[105]

Liquid subcooling

The rate of the convective heat transfer increases with liquid subcooling. As a result, liquid subcooling influences the inception and partial nucleate boiling regions of the boiling curve. On a wall flux *versus* wall superheat plot, convective heat flux and partial nucleate boiling curves lie higher than those for saturated

boiling. However, at high nucleate boiling heat fluxes, the subcooled and saturated boiling curves almost overlap. This behavior suggests that at high heat fluxes the convective contribution becomes small. Also, since the nucleation site density depends only on wall superheat, the number density of active sites must be playing an important role. At present no theoretical criterion such as that developed by Moissis and Berenson[38] for saturated boiling exists for transition from partial to fully developed nucleate boiling under subcooled conditions. The maximum heat flux is found to increase with subcooling. Zuber et al.[106] extended Equation 39 to a subcooled liquid by accounting for heat lost to the liquid in a transient manner. Their expression for maximum heat flux in subcooled liquids is

$$\frac{q_{max,sub}}{q_{max}} = [1 + C_1(g(\rho_L - \rho_G)\rho_G^2 a_L^4/\sigma^3)^{1/8}\,\mathrm{Ja}] \tag{57}$$

where q_{max} is the maximum heat flux given by Equation 39 for saturated liquids. From analysis, the constant, C_1, was found to have a value of 5.33. The Jakob number was defined in the same manner as given in Equation 9 except that ΔT was replaced by liquid subcooling, ΔT_{sub}. According to Equation 57, maximum heat flux increases linearly with subcooling. The prediction from Equation 57 was found to be in good agreement with subcooled water data obtained up to 2 atm and subcooled ethanol data obtained up to 10 atm.

Very recently Elkassabgi and Lienhard[107] have made an extensive investigation of maximum heat fluxes in subcooled pool boiling on horizontal cylinders. In the experiments, acetone, isopropanol, methanol, and Freon 113 were used as the test liquids and liquid subcoolings as high as 140°C were attained. Figure 23 shows their data obtained with isopropanol. Based on the trend of the data, three subcooling regimes for the maximum heat flux were identified. The data that varied linearly with subcooling (low subcooling) were correlated in a manner similar to Equation 57, but the time constant for transient liquid contacts was obtained from the mechanical energy stability criterion. Their correlation for low subcooling is

$$\frac{q_{max,sub}}{q_{max}} = 1 + 4.28\,\mathrm{Ja}/\mathrm{Pe}^{1/4} \tag{58}$$

where Peclet number is defined as negative one fourth power of the expression contained in the rounded parenthesis in Equation 57. The constant in Equation 58 was found to be independent of dimensionless cylinder radius. The maximum heat flux, q_{max}, in saturated boiling was obtained from the hydrodynamic predictions shown in Figure 8.

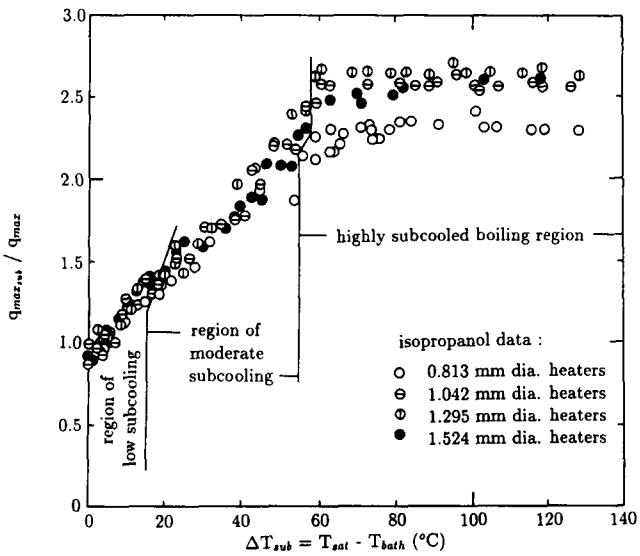

Figure 23 Maximum heat fluxes obtained during subcooled pool boiling on cylinders[107]

At moderate subcoolings, bubbles were observed to surround the heater without detaching. For these subcoolings, the maximum heat flux was considered to be determined by natural convection from the outer edge of the bubble boundary layer. Their correlation for moderate subcoolings is

$$\frac{q_{max,sub}}{(k_L/2R_{eff}\cdot\Delta T_{sub})} = 28 + 1.5\mathrm{Ra}^{1/4}/(\beta\,\Delta T_{sub})^{7/8} \tag{59}$$

where

$$\mathrm{Ra} \equiv \frac{g\beta\,\Delta T_{sub}(2R_{eff})^3}{a_L\nu_L} \tag{60}$$

$$\mathrm{R}_{eff} = R(1 + D_d/R) \tag{61}$$

where R is cylinder radius and D_d is given by Equation 10.

At very high subcoolings, the maximum heat flux was independent of ΔT_{sub}. Elkassabgi and Lienhard noted that the maximum heat flux was limited by the evaporation rate at the heater surface (the authors called it a molecular effusion limit) and not by the rate at which energy could be removed from the bubble boundary by natural convection. The maximum heat flux was correlated as

$$q_{max,sub} = \rho_G h_{LG}\sqrt{R_G T_{sat}/2\pi} \cdot[0.01 + 0.0047\exp(-1.11\times10^{-6}x)] \tag{62}$$

where

$$x = R(R_G T_{sat})^{1/2}/a_L \tag{63}$$

Equation 58 of Elkassabgi and Lienhard shows a much weaker dependence on Pe than Equation 57 of Zuber et al.[106] Since geometry influences the convective process, and the radius of the cylinder is used as the characteristic length for the molecular effusion limit, Equations 59 and 62 should be considered specific to the range of cylinder diameters employed in the study.

Transition boiling is influenced strongly by liquid subcooling. Very limited data on subcooled transition boiling is available in the literature. Figure 24 shows the transition boiling data obtained by Dhir[108] during quenching of a 19-mm diameter copper sphere in subcooled water. With increase in subcooling, the transition boiling curves move up and to the right. The maximum heat flux increases with subcooling. Though the maximum heat flux data varied somewhat nonlinearly with subcooling, it was found to correlate with Equation 57 when the constant C_1 was chosen have a value of 6.33 to account for the spherical geometry of the heater. In the transient cooling experiments, the nucleate boiling curves did not collapse on one curve.

External flow boiling

Flow velocity represents another variable that can significantly influence the boiling curve. Boiling under forced flow conditions can be divided into two categories: external and internal flow boiling. In this review only external flow boiling on surfaces is considered while an occasional reference has been made to boiling in tubes or channels (internal boiling). Since convective flow and heat transfer are affected by the geometry of the heater as well, both flow velocity and geometry interact to alter the boiling incipience and partial nucleate boiling heat transfer. An example of this behavior can be seen in Figure 17 in which the distribution of the partial nucleate boiling heat transfer coefficient around a horizontal tube is plotted. Generally liquid velocity

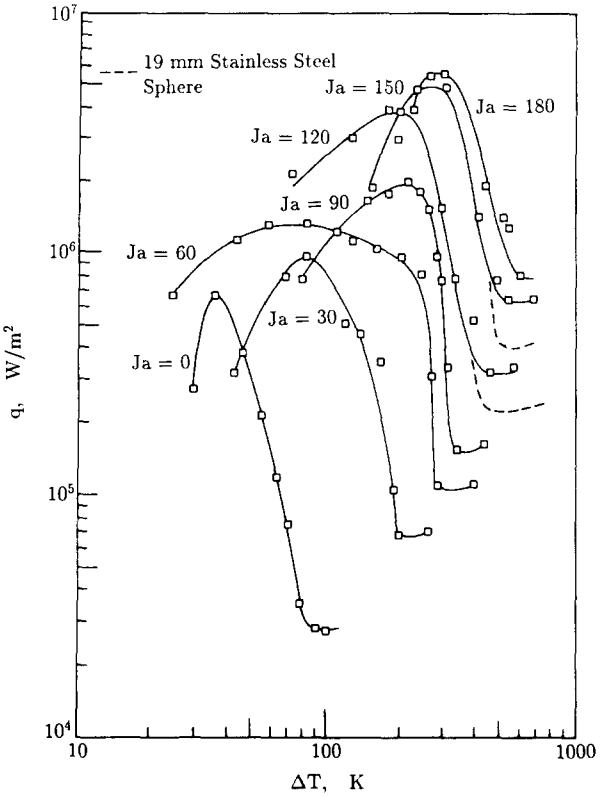

Figure 24 Effect of liquid subcooling on transition boiling curves obtained during quenching of spheres

enhances the incipience and the partial nucleate boiling heat fluxes. In fully developed nucleate boiling, however, velocity has little effect except that maximum heat flux increases with flow velocity. This effect of liquid velocity on nucleate boiling is similar to that of liquid subcooling. It should be noted though, that the preceding statement is true only as long as liquid inertia dominates the process.

Two of the most studied geometries under external flow conditions are those of a liquid jet impinging on a horizontal surface and that of flow normal to a horizontal cylinder. In the two cases the flow can be along the direction of gravity, against the direction of gravity, or normal to gravity. Fully developed nucleate boiling data of Katto and Monde[109] obtained with a saturated water jet issuing from a 2-mm diameter nozzle and impinging on an upward-facing electrically heated 8 × 8 mm stainless steel foil showed little effect of velocity. The pool and forced flow nucleate boiling data of Katto and Monde for the same configuration are shown in Figure 25. In a certain band, the nucleate boiling data obtained with an impinging jet is seen to lie on an extension of the pool boiling curve. The scatter in the pool boiling data was thought to have resulted from the fact that a new foil was used after each run. Semitheoretical correlations for the maximum heat flux obtained with impinging jets have been developed by Katto and Shimizu,[110] Monde,[111] and Sharan and Lienhard.[112] Monde extended the critical liquid layer model of Haramura and Katto, whereas Sharan and Lienhard's work had as its basis the mechanical energy stability criterion initially proposed by Lienhard and Eichhorn.[113] According to the mechanical energy stability criterion, the maximum heat flux occurs when the rate at which kinetic energy added to the coolant (as a result of evaporation) exceeds the rate at which energy is consumed in the formation of new droplets. The correlations of Monde[111] and Sharan and Lienhard[112] yield comparable results except at moderate-to-high pressures. More recently, Kato and Yokoya[114] have systematically evaluated all of the available data and have suggested a generalized correlation for the maximum heat flux on a horizontal disk cooled by an impinging jet as

$$\frac{q_{max}}{\rho_L U_L h_{LG}} = K\left[\frac{\sigma\rho_l}{(\rho_L U_L)^2(D-d)} - \frac{1}{(1+D/d)}\right]^m \tag{64}$$

where

$$K = 0.0166 + 7.00\left(\frac{\rho_G}{\rho_L}\right)^{1.12} \tag{65}$$

and

$$m = 0.374(\rho_G/\rho_L)^{0.0155} \quad \text{for} \quad \rho_G/\rho_L \le 0.00403 \tag{66}$$

$$m = 0.532(\rho_G/\rho_L)^{0.0794} \quad \text{for} \quad \rho_G/\rho_L \ge 0.00403 \tag{67}$$

In Equation 64 U_L is the liquid velocity. Equation 64, which is applicable to both an upward- and a downward-facing disk, is valid only as long as liquid supply rate from the nozzle is much higher than the evaporation rate at the heater surface.

The history of developments in the area of prediction of the maximum heat flux on cylinders has recently been reviewed by Leinhard.[54] Through several sequential modifications to the original mechanical stability criterion, Lienhard and coworkers have developed an expression for the maximum heat flux on nonalternating current (AC) heated cylinders in cross flow of saturated liquids as

$$\phi_{Pred} = \eta + \left[\frac{4\eta^2}{We_G}\left(1 - \sqrt{\phi_{Pred}(\phi_{Pred} - \eta)}\left(\frac{We_G^2}{6\eta^3}\right)\right)\right]^{1/3} \tag{68}$$

where

$$\phi = \frac{\pi q_{max}}{U_L \rho_G h_{LG}} \tag{69}$$

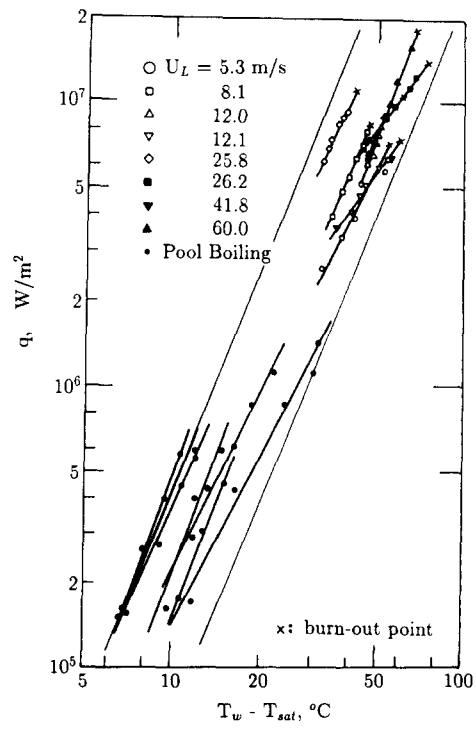

Figure 25 Comparison of pool and forced flow nucleate boiling data obtained on horizontal disks

$$\eta = 0.077 r^{0.314} \mathrm{We}_G^{-0.12} \tag{70}$$

$$r = \frac{\rho_L}{\rho_G} \tag{71}$$

$$\mathrm{We}_G = \frac{2R\rho_G U_L^2}{\sigma} \tag{72}$$

$$\mathrm{Fr} = \frac{U_L}{\sqrt{2Rg}} \tag{73}$$

Equation 68 is valid only for gravity-uninfluenced data (upflow, downflow, or normal) and for this case $\phi = \phi_{\mathrm{Pred}}$. The criterion for the data that are influenced by gravity is

$$r^{1.7}/\mathrm{Fr} \leq 3{,}000 \tag{74}$$

The gravity-influenced data were correlated as

$$\frac{\phi}{\phi_{\mathrm{Pred}}} = 1 + 2 \times 10^{-5} r^{1.7}/\mathrm{Fr} \tag{75}$$

Figure 26 shows the correlation and the data obtained under the influence of gravity and in the absence of it. It is seen that gravity-influenced data show a considerable scatter about the prediction made from the correlation. One reason for the scatter could be that the correlation does not take into account the local condition at the heater surface. It has been shown by Meyer et al.[115] that at low velocities, interaction between gravity and inertia can create a dead region for bubble movement and thereby can lead to a premature burnout.

A correlation for maximum heat fluxes for low velocity up flow across cylinders has also been developed by Ungar and Eichhorn.[116] By combining the sheet instability criterion with the mechanical instability criterion they were able to obtain the pertinent dimensionless groups for correlation of the data. The correlation of Ungar and Eichhorn is somewhat simpler to use than Equations 68 and 75.

If cross flow occurs over a bank of tubes, the data of Jensen and Hsu[117] for up flow show that nucleate boiling heat transfer coefficients are influenced by the location of the tube in the bundle. Because of accumulation of vapor along the flow direction, flow regimes change. A liquid film with vapor core was observed on tubes far away from the inlet. Thus, different types of burnout mechanisms may prevail in the lower and upper parts of a tube bundle. A thorough review of cross flow boiling on horizontal tube banks has been given by Jensen.[118]

A study of transient transition boiling on a hot horizontal surface cooled by an impinging jet has been reported by Ishigai et al.[119] This transient data show that high flow velocity and liquid subcooling shift the transition bonding curves upward and to the right. Their transition boiling curves showed some distortion and in some instances transition boiling heat fluxes over a certain range of surface temperatures were found to be independent of wall superheat. A similar behavior was observed by Dhir[108] during forced flow transient cooling of spheres. It should be mentioned that at low velocities Auracher[73] did not observe any effect of velocity on transition boiling.

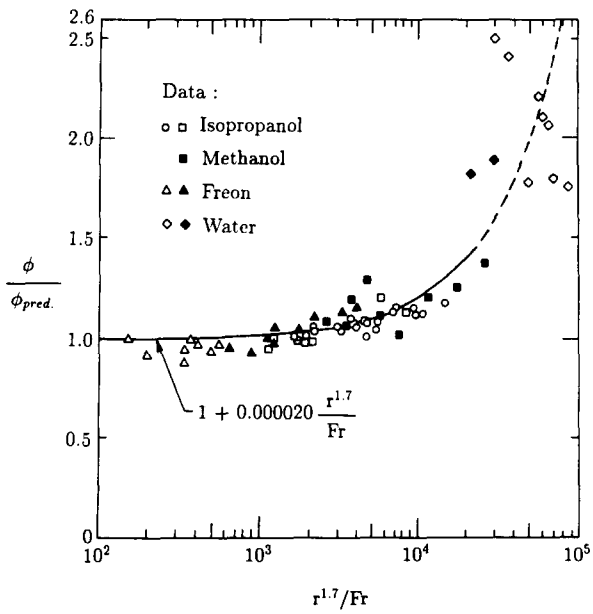

Figure 26 Correlation of maximum heat flux on horizontal cylinders subjected to forced flow of saturated liquids[54]

Future directions

In the last half century of boiling research we have made significant progress toward an understanding of the process. Very often this understanding is reflected in the form of semitheoretical correlations. The correlations serve an important purpose in providing predictions for geometries and flow conditions of interest. However, we are a long way from making a totally theoretical prediction of nucleate and transition boiling heat fluxes. The boiling process is an aggregate of many subprocesses and their interactions. The subprocesses are affected by many system variables (a few of which were included in the earlier discussion). Some of these subprocesses are better understood than others. But when it comes to the interactions of the subprocesses our understanding is very limited. One of the key unresolved issues in the prediction of nucleate and transition boiling heat fluxes is the knowledge of the density of active nucleation sites and the relation between active cavities and the cavities that are formed on the surface after the surface is prepared by following a certain procedure. Consideration must also be given to characterization of the surface (wettability, roughness, cavity size distribution and shape, etc.) and the wall void fraction in the fully developed nucleate and transition boiling. We also need to understand the mechanics of microlayer evaporation when the thickness of the microlayer is of the same order of magnitude as the rms value of surface roughness.

As we enter the second half century of boiling research it may be prudent to go back to very basic experiments. The experiments should be conducted on simple geometries and should initially involve as few variables as possible. One of the requirements of these experiments should be that macroscopic information must accompany as much microscopic data as possible. Available instrumentation may be inadequate for this purpose. Emphasis may therefore have to be placed on the development of new measurement techniques. A diligent effort has to be made to provide detailed information so that hypotheses made in the development of models are proved with little doubt. A starting point in this direction could be the repetition of experiments similar to those of Gaertner and Westwater but under much more controlled conditions and with additional instrumentation.

The experimental effort should be complemented with theoretical work. The process is highly nonlinear and to include detailed models of all the subprocesses and their interactions, perhaps we have no choice but to develop comprehensive computer codes. The computer models, if developed, should be totally mechanistic and should to the extent possible be free of adjustable parameters.

Acknowledgment

The work was supported by the National Science Foundation under grant CBT 8821447.

References

1 Nukiyama, S. The maximum and minimum values of the heat Q transmitted from metal to boiling water under atmospheric pressure. *J. JSME*, 1934, **37**, 367–374 (Reprinted in *Int. J. Heat Mass Transfer*, 1966, **9**, 1419–1433)
2 Kenning, D. B. R. Pool boiling. *Two Phase Flow and Heat Transfer*, D. Butterworth and G. F. Hewitt, eds. Oxford University Press, Oxford, 1977, 128–152
3 Fujita, Y. Recent developments in pool boiling heat transfer. *Proc. 4th Int. Topical Meeting on Nuclear Reactor Thermal Hydraulics*, Karlsruhe, Germany, 1989, **2**, 1068–1086
4 Bankoff, S. G. Entrainment of gas in the spreading of a liquid over a rough surface. *AIChE J.*, 1958, **4**, 24–26
5 Clark, H. B., Strenge, P. S., and Westwater, J. W. Active sites for nucleation. *Chem. Engr. Prog. Symp. Series*, 1959, **55**, 103–110
6 Hsu, Y. Y. On the size range of active nucleation cavities on a heating surface. *ASME J. Heat Transfer, 1962*, **84**, 207–216
7 Hsu, Y. Y., and Graham, R. W. *Transport Processes in Boiling and Two Phase Systems*. Hemisphere Publishing Corp., Washington, DC, 1976
8 Mizukami, K. The effect of gases on the stability and nucleation of vapor bubble nuclei. *Letters in Heat and Mass Transfer*, 1977, **4**, 17–26
9 Nishio, S. Stability of pre-existing vapor nucleus in uniform temperature field. *Trans. JSME B*, 1985, **54-503**, 1802
10 Kenning, D. B. R. Wall temperatures in nucleate boiling. *Proc. Eurotherm. Seminar No. 8 on Advances in Pool Boiling Heat Transfer*, Paderborn, Germany, 1989, 1–9
11 Mikic, B. B., and Rohsenow, W. M. A new correlation of pool boiling data including the effect of heating surface characteristics. *ASME J. Heat Transfer*, 1969, **9**, 245–250
12 Plesset, M. S., and Zwick, S. A. Growth of vapor bubbles in superheated liquids. *J. Appl. Phys.*, 1954, **25**, 493–500
13 Mikic, B. B., Rohsenow, W. M., and Griffith, P. On bubble growth rates. *Int. J. Heat and Mass Transfer*, 1970, **13**, 657–666
14 Snyder, N. R., and Edwards, D. K. Summary of conference on bubble dynamics and boiling heat transfer. Memo 20-137, Jet Propulsion Laboratory. Pasadena, CA, USA, 1956, 14–15
15 Moore, F. D., and Mesler, R. B. The measurement of rapid surface temperature fluctuations during nucleate boiling of water. *AIChE J.*, 1961, **7**, 620–624
16 Fritz, W. Maximum volume of vapor bubbles. *Physik Zeitschr.*, 1935, **36**, 379–384
17 Cooper, M. G., Judd, A. M., and Pike, R. A. Shape and departure of single bubbles growing at a wall. *Proc. 6th Int. Heat Transfer Conf.*, Toronto, Ontario, Canada, 1978, **1**, 115–120
18 Cole, R., and Rohsenow, W. Correlations of bubble departure diameters for boiling of saturated liquids. *Chem. Engr. Prog.*, 1969, **65**, 211–213
19 Gorenflo, D., Knabe, V., and Bieling, V. Bubble density on surfaces with nucleate boiling—its influence on heat transfer, and burnout heat flux at elevated saturation pressures. *Proc. 8th Int. Heat Transfer Conf.*, San Francisco, CA, USA, 1986, **4**, 1995–2000
20 Moalem, D., Zijl, W., and van Stralen, S. J. D. Nucleate boiling at a liquid–liquid interface. *Letters Heat and Mass Transfer*, 1977, **4**, 319–329
21 Cole, R., and van Stralen, S. J. D. *Boiling Phenomena*. Hemisphere Publishing Corp., Washington, DC, 1979
22 Han, C. Y., and Griffith, P. The mechanism of heat transfer in nucleate pool boiling. Part I. Bubble initiation, growth and departure. *Int. J. Heat and Mass Transfer*, 1965, **8**, 887–904
23 Malenkov, I. G. Detachment frequency as a function of size of vapor bubbles (translated). *Inzh. Fiz. Zhur.*, 1971, **20**, 99
24 Gaertner, R. F., and Westwater, J. W. Population of active sites in nucleate boiling heat transfer. *Chem. Engr. Prog. Symp. Series*, 1960, **56**, 39–48
25 Sultan, M., and Judd, R. L. Spatial distribution of active sites and bubble flux density. *ASME J. Heat Transfer*, 1978, **100**, 56–62
26 Cornwell, K., and Brown, R. D. Boiling surface topography. *Proc. 6th Int. Heat Transfer Conf.*, Toronto, Ontario, Canada, 1978, **1**, 157–161
27 Singh, A., Mikic, B. B., and Rohsenow, W. Relative behavior of water and organics in boiling. *Proc. 6th Int. Heat Transfer Conf.*, Toronto, Ontario, Canada, 1978, **1**, 163–168
28 Kocamustafaogullari, G., Ishii, M. Interfacial area and nucleation site density in boiling systems. *Int. J. Heat and Mass Transfer*, 1983, **26**, 1377–1387
29 Bier, K., Gorenflo, D., Salem, M., and Tanes, Y. Pool boiling heat transfer and size of active nucleation centers for horizontal plates with different surface roughness. *Proc. 6th Int. Heat Transfer Conf.*, Toronto, Ontario, Canada, 1968, **1**, 151–156
30 Yang, S. R., and Kim, R. H. A mathematical model of the pool boiling nucleation site density in terms of the surface characteristics. *Int. J. Heat and Mass Transfer*, 1988, **31**, 1127–1135
31 Gaertner, R. F. Distribution of active sites in the nucleate boiling of liquids. *Chem. Engr. Prog. Symp. Series*, 1963, **59**, 52–61
32 Eddington, R. I., Kenning, D. B. R., and Korneichev, A. I. Comparison of gas and vapor bubble nucleation on a brass surface in water. *Int. J. Heat and Mass Transfer*, 1978, **21**, 855–862
33 Eddington, R. I., and Kenning, D. B. R. The prediction of flow boiling bubble populations from gas bubble nucleation experiments. *Proc. 6th Int. Heat Transfer Conf.*, Toronto, Ontario, Canada, 1978, **1**, 275–280
34 Sultan, M., and Judd, R. L. Interaction of the nucleation phenomena at adjacent sites in nucleate boiling. *ASME J. Heat Transfer*, 1983, **105**, 3–9
35 Judd, R. L. On nucleation site interaction. *ASME J. Heat Transfer*, 1988, **110**, 475–478
36 Gaertner, R. F. Photographic study of nucleate pool boiling on a horizontal surface. *ASME J. Heat Transfer*, 1965, **87**, 17–29
37 Zuber, N. Hydrodynamic aspects of boiling heat transfer. Ph.D. Thesis, University of California, Los Angeles, CA, USA (also published as USAEC Report No. AECU-4439)
38 Moissis, R., and Berenson, P. J. On the hydrodynamic transitions in nucleate boiling. *ASME J. Heat Transfer*, 1963, **85**, 221–229
39 Nishikawa, K., Fujita, Y., and Ohta, H. Effect of surface configuration on nucleate boiling heat transfer. *Int. J. Heat and Mass Transfer*, 1974, **27**, 1559–1571
40 Forster, D. E., and Greif, R. Heat transfer to a boiling liquid—mechanism and correlation. *ASME J. Heat Transfer*, 1959, **81**, 43–53
41 Rohsenow, W. M. Boiling. In *Handbook of Heat Transfer Fundamentals*, 2nd ed, W. M. Rohsenow, J. P. Hartnett, and E. N. Ganic, eds. McGraw-Hill, New York, 1985, 12-1–12-4
42 Judd, R. L., and Hwang, K. S. A comprehensive model for nucleate pool boiling heat transfer including microlayer evaporation. *ASME J. Heat Transfer*, 1976, **98**, 623–629
43 Paul, D. D., and Abdel-Khalik, S. I. A statistical analysis of saturated nucleate boiling along a heated wire. *Int. J. Heat and Mass Transfer*, 1983, **26**, 509–519
44 Fath, H. S., and Judd, R. L. Influence of system pressure on microlayer evaporation heat transfer. *ASME J. Heat Transfer*, 1978, **100**, 49–55
45 Bobst, R. W., and Colver, C. P. Temperature profiles up to burnout adjacent to a horizontal heating surface in nucleate pool boiling of water. *Chem. Eng. Prog. Symp. Series*, 1968, **64**, 26–32
46 Iida, Y., and Kobayasi, K. Distribution of void fraction above a horizontal heating surface in pool boiling. *Bull. JSME*, 1969, **12**, 283–290
47 Liaw, S. P., and Dhir, V. K. Void fraction measurements during saturated pool boiling of water on partially wetted vertical surfaces. *ASME J. Heat Transfer*, 1989, **111**, 731–738
48 Bhat, A. M., Saini, J. S., and Prakash, R. Role of macrolayer evaporation in pool boiling at high heat flux. *Int. J. Heat and Mass Transfer*, 1986, **29**, 1953–1961
49 Bhat, A. M., Prakash, R., and Saini, J. S. On the mechanism

of macrolayer formation in nucleate pool boiling at high heat flux. *Int. J. Heat and Mass Transfer*, 1983, **26**, 735–740
50 Bhat, A. M., Prakash, R., and Saini, J. S. Heat transfer in nucleate pool boiling at high heat flux. *Int. J. Heat and Mass Transfer*, 1983, **26**, 833–840
51 Dhir, V. K., and Liaw, S. P. Framework for a unified model for nucleate and transition pool boiling. *ASME J. Heat Transfer*, 1989, **111**, 739–746
52 Kutateladze, S. S. On the transition to film boiling under natural convection. *Kotlo-turbostoenie*, 1948, **3**, 10
53 Lienhard, J. H., and Dhir, V. K. Extended hydrodynamic theory of the peak and minimum pool boiling heat fluxes. *NASA* CR-2270, 1973
54 Lienhard, J. H. Burnout on cylinders. *ASME J. Heat Transfer*, 1988, **110**, 1271–1286
55 Dhir, V. K., and Lienhard, J. H. Peak pool boiling heat flux in viscous liquids. *ASME J. Heat Transfer*, 1974, **96**, 71–78
56 Costello, C. P., and Frea, W. J. A salient non-hydrodynamic effect in pool boiling burnout of small semi-cylinder heaters. *Chem. Eng. Prog. Symp. Series*, 1965, **61**, 258–268
57 Costello, C. P., Bock, C. O., and Nichols, C. C. A study of induced convective effects on pool boiling burnout. *Chem. Eng. Prog. Symp. Series*, 1965, **61**, 271–280
58 Lienhard, J. H., Dhir, V. K., and Rieherd, D. M. Peak pool boiling heat flux measurements on finite horizontal flat plates. *ASME J. Heat Transfer*, 1974, **95**, 477–482
59 Hasegawa, S., Echigo, R., and Takegawa, T. Maximum heat fluxes for pool boiling on partly ill-wettable heating surfaces. *Bull. JSME*, 1973, **96**, 1076–1084
60 Liaw, S. P., and Dhir, V. K. Effect of surface wettability on transition boiling heat transfer from a vertical surface. *Proc. 8th Int. Heat Transfer Conf.*, San Francisco, CA, USA, 1986, **4**, 2031–2036
61 Hahne, E., and Diesselhorst, T. Hydrodynamic and surface effects on the peak heat flux in pool boiling. *Proc. 6th Int. Heat Transfer Conf.*, Toronto, Ontario, Canada, 1978, **1**, 209–219
62 Maracy, M., and Winterton, R. H. S. Hysteresis and contact angle effects in transition pool boiling of water. *Int. J. Heat and Mass Transfer*, 1988, **31**, 1443–1449
63 Haramura, Y., and Katto, Y. A new hydrodynamic model of critical heat flux, applicable widely to both pool and forced convection boiling on submerged bodies in saturated liquids. *Int. J. Heat and Mass Transfer*, 1983, **26**, 389–399
64 Pasamehmetoglu, K. O., and Nelson, R. A. The effect of Helmholtz instability on the macrolayer thickness in vapor mushroom region of nucleate pool boiling. *Int. Comm. Heat and Mass Transfer*, 1987, **14**, 709–720
65 Drew, T. B., and Mueller, C. Boiling. *Trans. Am. Inst. Chem. Eng.*, 1937, **33**, 449–473
66 Berenson, P. J. Experiments on pool boiling heat transfer. *Int. J. Heat and Mass Transfer*, 1962, **5**, 985–999
67 Stephan, K. Ubertragung hoher warmestromelichten au siedenee flussigkeiten. *Chemie Ingr. Tech.* 1966, **38**, 112–117
68 Kovalev, S. A. On methods of studying heat transfer in transition boiling. *Int. J. Heat and Mass Transfer*, 1968, **11**, 279–283
69 Hesse, G. Heat transfer in nucleate boiling, maximum heat flux and transition boiling. *Int. J. Heat and Mass Transfer*, 1973, **16**, 1611–1627
70 Ramilison, J. M., and Leinhard, J. H. Transition boiling heat transfer and the film transition regime. *ASME J. Heat Transfer*, 1987, **109**, 746–752
71 Peterson, W. C., and Zallouk, M. G. Boiling curve measurements from a controlled heat transfer process. *ASME J. Heat Transfer*, 1971, **93**, 406–412
72 Sakurai, A., and Shiotsu, M. Temperature controlled pool boiling heat transfer. *Proc. 5th Int. Heat Transfer Conf.*, Tokyo, Japan, 1974, **4**, 81–85
73 Auracher, H. Similarities between nucleate and transition boiling under natural and forced convection conditions advances in pool boiling heat transfer. *Proc. Eurotherm. Seminar No. 8 on Advances in Pool Boiling Heat Transfer*, Paderborn, Germany, 1989, pp. 82–85
74 Kalinin, E. K., Berlin, I. T., Kostyuk, V. V., and Nosova, E. M. Heat transfer during transition boiling of cryogenic liquids. *Advances in Cryogenic Engineering*, 1976, **21**, 273–277
75 Bjornard, T. A., and Griffith, P. PWR blowdown heat transfer. *Symp. on the Thermal and Hydraulic Aspects of Nuclear Reactor Safety*, O. C. Jones, ed. The ASME Winter Annual Meeting, 1977, **1** (Light Water Reactors), 17–39
76 Hsu, Y. Y., and Kim, E. S. Transition boiling. *Int. Comm. Heat and Mass Transfer*, 1988, **15**, 533–558
77 Nishikawa, K., Fujii, T., and Honda, A. Experimental study on the mechanisms of transition boiling heat transfer. *Bull. JSME*, 1972, **15**, 93–103
78 Ragheb, H. S., and Cheng, S. C. Surface wetted area during transition boiling in forced convective flow. *ASME J. Heat Transfer*, 1979, **101**, 381–383
79 Tong, L. S., and Young, J. D. A phenomenological transition and film boiling heat transfer correlation. *Proc. 5th Int. Heat Transfer Conf.*, Tokyo, Japan, 1974, **4**, 120–124
80 Dhuga, D. S., and Winterton, R. H. S. Measurement of surface contacts in transition boiling. *Int. J. Heat Mass Transfer*, 1985, **28**, 1869–1880
81 Dhuga, D. S., and Winterton, R. H. S. The pool boiling curve and liquid–solid contact. *Proc. 8th Int. Heat Transfer Conf.*, San Francisco, CA, USA, 1986, **4**, 2055–2060
82 Lee, Y. Y. W., Chen, J. C., and Nelson, R. A. Liquid–solid contact measurements using a surface thermocouple probe in atmospheric pool boiling water. *Int. J. Heat and Mass Transfer*, 1985, **28**, 1415–1423
83 Witte, L. C., and Leinhard, J. H. On the existence of two 'transition' boiling curves. *Int. J. Heat Mass Transfer*, 1982, **25**, 771–779
84 Bui, T. D., and Dhir, V. K. Transition boiling heat transfer on a vertical surface. *ASME J. Heat Transfer*, 1985, **107**, 756–763
85 Shoukri, M., and Judd, R. L. On the influence of surface conditions in nucleate boiling—the concept of bubble flux density. *ASME J. Heat Transfer*, 1978, **100**, 618–623
86 Joudi, K. A., and James, D. D. Surface contamination, rejuvenation, and the reproducibility of results in nucleate pool boiling. *J. Heat Transfer*, 1981, **103**, 453–458
87 Ross, T. K. Corrosion and heat transfer—a review. *Br. Corros. J.* 1967, **2**, 131–142
88 Lance, R. P., and Myers, J. E. Local boiling coefficients on a horizontal tube. *AIChE J.*, 1950, **4**, 75–80
89 Cornwell, K., and Einarsson, J. G. The influence of fluid flow on nucleate boiling from a tube. *Proc. Eurotherm Seminar No. 8 on Advances in Pool Boiling Heat Transfer*, Paderborn, Germany, 1989, 28–41
90 Houchin, W. R., and Lienhard, J. H. Boiling burnout in low thermal capacity heaters. *ASME* Paper No. 66-WA/HT-40, 1966
91 Tachibana, F., Akiyama, M., and Kawamura, H. Non-hydrodynamic aspects of pool boiling burnout. *J. Nucl. Sci. and Tech.* 1967, **4**, 121–130
92 Merte, H. Nucleate pool boiling: high gravity to reduced gravity; liquid metals to cryogenics. *Trans. 5th Symp. Space Nuclear Power Systems*, Albuquerque, NM, USA, 1988, 437–442
93 Zell, M., Straub, J., and Vogel, B. Pool boiling under microgravity. *Proc. Eurotherm Seminar No. 8 on Advances in Pool Boiling Heat Transfer*, Paderborn, Germany, 1989, 70–74
94 Siegel, R., and Usiskin, C. A photographic study of boiling in the absence of gravity. *ASME J. Heat Transfer*, 1959, **81**, 230–238
95 Johnson, H. A. Transient boiling heat transfer to water. *Int. J. Heat and Mass Transfer*, 1971, **14**, 67–82
96 Sakurai, A., and Shiotsu, M. Transient pool boiling heat transfer. Part 1. Incipience boiling superheat. *ASME J. Heat Transfer*, 1977, **99**, 547–553
97 Sakurai, A., and Shiotsu, M. Transient pool boiling heat transfer. Part 2. Boiling heat transfer and burnout. *ASME J. Heat Transfer*, 1977, **99**, 554–560
98 Kozawa, Y., Inoue, T., and Okuyama, K. Enhancement of bubble formation and heat removal in transient boiling. *Proc. 8th Int. Heat Transfer Conf.*, San Francisco, CA, USA, 1986, **4**, 2007–2012
99 Serizawa, A. Theoretical prediction of maximum heat flux in power transients. *Int. J. Heat and Mass Transfer*, 1983, **26**, 921–932
100 Pasamehmetoglu, K. O., Nelson, R. A., and Gunnersonn, F. A theoretical prediction of critical heat flux in saturated pool

boiling during power transients. *ASME HTD*, 1987, **77**, 57–64
101 Bergles, A. E., and Thompson, Jr., W. G. The relationship of quench data to steady state pool boiling data. *Int. J. Heat and Mass Transfer*, 1970, **13**, 55–68
102 Veres, D. R., and Florschuetz, L. W. A comparison of transient and steady state pool boiling data obtained using the same heating surface. *ASME J. Heat Transfer*, 1971, **93**, 229–232
103 Peyayopanakul, W., and Westwater, J. W. Evaluation of the unsteady state quenching method for determining boiling curves. *Int. J. Heat and Mass Transfer*, 1978, **21**, 1437–1445
104 Lin, D. Y. T., and Westwater, J. W. Effect of metal thermal properties on boiling curves obtained by the quenching method. *Proc. 7th Int. Heat Transfer Conf.*, Munich, Germany, 1982, **4**, 155–160
105 Irving, M. E., and Westwater, J. W. Limitations for obtaining boiling curves by the quenching method with spheres. *Proc. 8th Int. Heat Transfer Conf.*, San Francisco, CA, USA, 1986, **4**, 2061–2066
106 Zuber, M., Tribus, M., and Westwater, J. W. The hydrodynamic crisis in pool boiling of saturated liquids. *Proc. 2nd Int. Heat Transfer Conf.*, Denver, CO, USA, 1961, 27
107 Elkassabgi, Y., and Lienhard, J. H. The peak pool boiling heat flux from horizontal cylinders in subcooled liquids. *ASME J. Heat Transfer*, 1988, **110**, 479–486
108 Dhir, V. K. Study of transient boiling heat fluxes from spheres subjected to forced vertical flow. *Proc. 6th Int. Heat Transfer Conf.*, Toronto, Ontario, Canada, 1978, **4**, 451–456
109 Katto, Y., and Monde, M. Study of mechanism of burn-out in a high heat flux boiling system with an impinging jet. *Proc. 5th Int. Heat Transfer Conf.*, Tokyo, Japan, 1974, **4**, 245–249
110 Katto, Y., and Shimizu, M. Upper limit of CHF in the saturated forced convection boiling on a heated disk with a small impinging jet. *ASME J. Heat Transfer*, 1979, **101**, 265–269
111 Monde, M. Critical heat flux in saturated forced convection boiling on a heated disk with an impinging jet. *ASME J. Heat Transfer*, 1987, **109**, 991–996
112 Sharan, A., and Lienhard, J. H. On predicting burnout in the jet configuration. *ASME J. Heat Transfer*, 1985, **107**, 398–401
113 Lienhard, J. H., and Eichhorn, R. On predicting boiling burnout for heaters cooled by liquid jets. *Int. J. Heat and Mass Transfer*, 1979, **22**, 774–776
114 Katto, Y., and Yokoya, S. Critical heat flux on a disk heater cooled by a circular jet of saturated liquid impinging at the center. *Int. J. Heat and Mass Transfer*, 1988, **31**, 219–227
115 Meyer, G., Gaddis, E. S., and Vogelpohl, A. Critical heat flux on a cylinder of large diameter in cross flow. *Proc. 8th Int. Heat Transfer Conf.*, San Francisco, CA, USA, 1986, **5**, 2125–2130
116 Ungar, E. K., and Eichhorn, R. A new hydrodynamic prediction of the peak heat flux from horizontal cylinders in low speed upflow. *Proc. ASME Heat Transfer Conf.*, Houston, TX, USA, 1988, **2**, 643–657
117 Jensen, M. K., and Hsu, J. T. A parametric study of boiling heat transfer in a horizontal tube bundle. *ASME J. Heat Transfer*, 1988, **110**, 976–981
118 Jensen, M. K. Boiling on the shellside of horizontal tube boilers. *Two Phase Heat Exchangers*, S. Kakac et al., eds. Kulwar Press, Boston, 1988, pp. 707–746
119 Ishigai, S., Nakanishi, S., and Ochi, T. Boiling heat transfer for a plane water jet impinging on a hot surface. *Proc. 6th Int. Heat Transfer Conf.*, Toronto, Ontario, Canada, 1978, **1**, 445–450